



**DEVELOPMENT OF A MOLECULAR HYBRID OF  
MICRORNA AND APTAMER FOR REGULATING THE  
PROLIFERATION OF COLORECTAL CANCER CELL**

**BY**

**KHANITTHA LAOWICHUWAKONNUKUL**

**A THESIS SUBMITTED IN PARTIAL FULFILLMENT  
OF THE REQUIREMENTS FOR THE DEGREE OF  
MASTER OF SCIENCE  
(BIOCHEMISTRY AND MOLECULAR BIOLOGY)  
FACULTY OF MEDICINE  
THAMMASAT UNIVERSITY  
ACADEMIC YEAR 2024**

**DEVELOPMENT OF A MOLECULAR HYBRID OF  
MICRORNA AND APTAMER FOR REGULATING THE  
PROLIFERATION OF COLORECTAL CANCER CELL**

**BY**

**KHANITTHA LAOWICHUWAKONNUKUL**

**A THESIS SUBMITTED IN PARTIAL FULFILLMENT  
OF THE REQUIREMENTS FOR THE DEGREE OF  
MASTER OF SCIENCE  
(BIOCHEMISTRY AND MOLECULAR BIOLOGY)  
FACULTY OF MEDICINE  
THAMMASAT UNIVERSITY  
ACADEMIC YEAR 2024**

THAMMASAT UNIVERSITY  
FACULTY OF MEDICINE

THESIS

BY

KHANITTHA LAOWICHUWAKONNUKUL

ENTITLED

DEVELOPMENT OF A MOLECULAR HYBRID OF MICRORNA AND  
APTAMER FOR REGULATING THE PROLIFERATION OF COLORECTAL  
CANCER CELL

was approved as partial fulfillment of the requirements for  
the degree of Master of Science (Biochemistry and Molecular Biology)

on March 21, 2025

Chairman

Kulthida V. Charn

(Associate Professor Kulthida Vaeteewoottacharn, Ph.D., M.D.)

Member and Advisor

Pichayanoot Rotkrua

(Assistant Professor Pichayanoot Rotkrua, Ph.D.)

Member and Co Advisor

B. Soontorn.

(Associate Professor Boonchoy Soontornworajit, Ph.D.)

Member

P. Tingpej

(Assistant Professor Pholawat Tingpej, Ph.D., M.D.)

Dean

Auchara Tangsathapornpong

(Associate Professor Auchara Tangsathapornpong, M.D.)

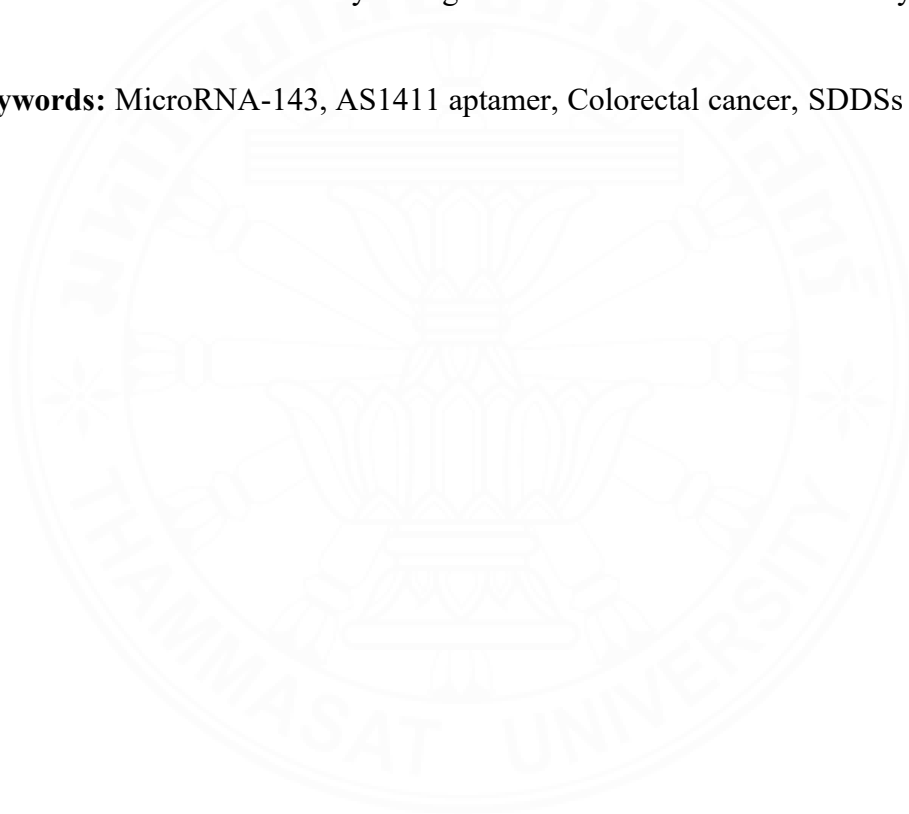
Thesis Title	DEVELOPMENT OF A MOLECULAR HYBRID OF MICRORNA AND APTAMER FOR REGULATING THE PROLIFERATION OF COLORECTAL CANCER CELL
Author	KHANITTHA LAOWICHUWAKONNUKUL
Degree	Master of Science
Major Field/Faculty/University	Biochemistry and Molecular Biology Faculty of Medicine Thammasat University
Thesis Advisor	Assistant Professor Pichayanoot Rotkrua, Ph.D.
Thesis Co-Advisor (If any)	Associate Professor Boonchoy Soontornworajit, Ph.D.
Academic Year	2024

## ABSTRACT

*KRAS* is considered to be the most common oncogenic gene in human cancers. *KRAS* mutations are found in approximately 50% of colorectal cancer (CRC), so *KRAS* is one of the therapeutic targets for cancer drug development. *KRAS* is well-known to be targeted by tumor-suppressor miR-143. An increase in miR-143 expression is a promising way to inhibit CRC cell growth. Besides, there are several limitations to existing treatment, including unwanted side effects. Smart drug delivery systems (SDDSs) are potential methods for improving treatment efficiency. This research aims to develop an anticancer drug carrier, a molecular hybrid (MAH). The MAH was produced by combining miR-143 and AS1411 aptamers through a hybridization strand and loading doxorubicin (Dox), a chemotherapy drug. The uptake capability of MAH into the CRC SW480 cells was confirmed by detecting fluorescence intensity with a fluorescence microscope. After treatment of MAH in SW480 cells, the expression levels of miR-143 and *KRAS* mRNA were detected using an RT-qPCR assay, while the *KRAS* protein level was measured using a western blot analysis. MTS assay was used to determine cell viability, and flow cytometry was performed to assess cell apoptosis following Dox-MAH treatment. The downstream target proteins of *KRAS*, ERK and AKT, and apoptosis-related proteins, procaspase-3, Bax and Bcl-2, were evaluated using a western blot analysis. The results revealed that the level of miR-

143 was increased, but KRAS expression was decreased for both mRNA and protein. ERK and AKT proteins were downregulated as well. Furthermore, treating cells with Dox-MAH resulted in the inhibition of cell proliferation and induction of apoptosis. The expression of procaspase-3 and Bcl-2 was decreased, while Bax was increased, confirming that Dox-MAH triggered the cell apoptosis. The success of this research proposed a new strategy for drug delivery systems. Dox-MAH had multiple functions simultaneously; CRC cell-specificity, Dox carrier, and miR-143 delivery. Therefore, therapeutic efficacy could be increased and off-target toxicity would be decreased due to SDDSs' ability to target cancer cells but not harm healthy cells.

**Keywords:** MicroRNA-143, AS1411 aptamer, Colorectal cancer, SDDSs



## ACKNOWLEDGEMENTS

I would like to express my sincere appreciation and gratitude to my advisor, Assist. Prof. Dr. Pichayanoot Rotkrua, and my co-advisor, Assoc. Prof. Dr. Boonchoy Soontornworajit for their excellent advice, continuous support, compassion, and encouragement. This research I conducted would not have been feasible without their constant assistance.

Furthermore, I would like to thank Assoc. Prof. Dr. Kulthida Vaeteewoottacharn and Assist. Prof. Dr. Pholawat Tingpej for their valuable comments and helpful suggestions, which greatly improved my research.

I am grateful to all the lab groups, my classmates, and the staff at the Faculty of Medicine for their assistance and friendship.

In addition, I would like to thank my family and friends for providing me with support and encouragement at every stage of my personal and academic life.

Finally, the authors gratefully acknowledge the financial support provided by the Faculty of Medicine, Thammasat University.

Thank you very much.

Khanittha Laowichuwakonnukul

## TABLE OF CONTENTS

	Page
ABSTRACT	(1)
ACKNOWLEDGEMENTS	(3)
LIST OF TABLES (If any)	(8)
LIST OF FIGURES (If any)	(9)
LIST OF ABBREVIATIONS (If any)	(12)
CHAPTER 1 INTRODUCTION	1
1.1 Research Problems	4
1.2 Objective	5
1.3 Outcome	5
CHAPTER 2 REVIEW OF LITERATURE	6
2.1 Colorectal cancer	6
2.2 Aptamer	7
2.2.1 Overview of aptamer	7
2.2.2 Application of aptamer	9
2.2.2.1 Aptamers as therapeutic agents	9
2.2.2.2 Aptamers in the diagnosis of diseases	9
2.2.2.3 Aptamer-drug conjugates (ApDCs) for targeted drug delivery	9
2.2.2.4 ApDCs for chemotherapy	10
2.2.2.5 ApDCs for gene therapy	11
2.2.3 AS1411 aptamer	11

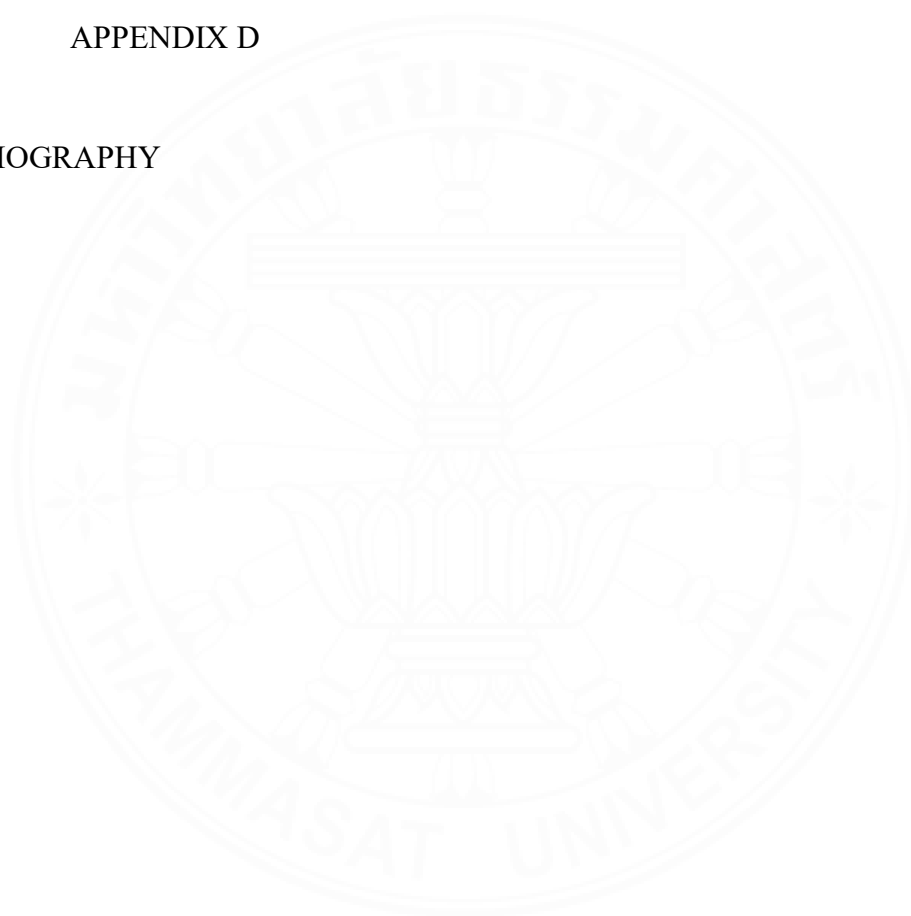
2.2.3.1 Overall of AS1411 aptamer	11
2.2.3.2 Application of AS1411 aptamer in cancer	12
2.3 MicroRNAs	13
2.3.1 MicroRNAs in cancer	13
2.3.2 MicroRNA-143	14
2.4 Doxorubicin	15
 CHAPTER 3 RESEARCH METHODOLOGY	 18
3.1 Chemicals and reagents	18
3.2 Instruments and lab equipment	19
3.3 Sequence design for miR-143, AS1411 aptamers, and a hybridization strand	20
3.4 Formation of molecular hybrid of miR-143 and AS1411 aptamer (MAH)	21
3.5 In vitro stability of MAH	21
3.6 Cell culture	21
3.7 Quantification of endogenous miR-143 in CRC and normal colon cell lines using RT-qPCR	21
3.8 In vitro cellular uptake of MAH	22
3.8.1 Study of AS1411 binding capability using a fluorescence microscope	22
3.8.2 RT-qPCR analysis of exogenous miR-143	22
3.9 Investigation of alteration of miR-143 target gene products	23
3.9.1 RT-qPCR analysis of KRAS mRNA	23
3.9.2 Western blot analysis of KRAS, ERK, and AKT proteins	23
3.10 Intercalation of Dox into MAH	24
3.11 CRC and normal colon cell proliferation assay after Dox- MAH treatment	24
3.12 Detection of CRC cell apoptosis after Dox-MAH treatment	25
3.13 Western blot analysis of procaspase-3, Bax and Bcl-2 proteins in the apoptosis pathway	25



3.14 Statistical analysis	25
CHAPTER 4 RESULTS AND DISCUSSION	26
4.1 Sequence design for aptamers, miR-143, and a hybridization strand	26
4.2 Formation of molecular hybrid of miR-143 and AS1411 aptamer (MAH)	27
4.3 <i>In vitro</i> stability of MAH	28
4.4 Quantification of endogenous miR-143 in CRC and normal colon cell lines using quantitative reverse transcription polymerase chain reaction (RT-qPCR)	29
4.5 <i>In vitro</i> cellular uptake of MAH	29
4.5.1 Study of AS1411 binding capability using a fluorescence microscope	29
4.5.2 RT-qPCR analysis of exogenous miR-143	31
4.6 Investigation of alteration of miR-143 target gene products	32
4.6.1 KRAS mRNA analysis using RT-qPCR in SW480 cells	32
4.6.2 KRAS mRNA analysis using RT-qPCR in CCD 841 CoN cells	33
4.6.3 Western blot analysis of KRAS, AKT and ERK proteins in SW480 cells	34
4.7 Intercalation of Dox into MAH	35
4.8 <i>In vitro</i> anti-proliferation studies	36
4.8.1 Effect of Dox-MAH on SW480	36
4.8.2 Effect of Dox-MAH on CCD 841 CoN	37
4.9 Detection of CRC cell apoptosis after Dox-MAH treatment	38
4.10 Western blot analysis of proteins in the relevant signaling pathways.	39

CHAPTER 5 CONCLUSIONS AND RECOMMENDATIONS	41
---	----

REFERENCES	43
APPENDICES	60
APPENDIX A	61
APPENDIX B	62
APPENDIX C	63
APPENDIX D	65
BIOGRAPHY	68



## LIST OF TABLES

Tables	Page
4.1 List of oligonucleotides and their modification	26



## LIST OF FIGURES

Figures	Page
1.1 Structure sketch of selective drug delivery systems (SDDS), Dox-Loaded Molecular Hybrid of miR-143 and AS1411 Aptamer (Dox-MAH).	3
1.2 When AS1411 aptamer binds to the nucleolin receptor on CRC cells, Dox-MAH is endocytosed, and then Dox and miR-143 are released into the cells.	4
2.1 The conventional processes of systematic evolution of ligands by exponential enrichment (SELEX).	8
2.2 Applications of aptamers in cancer therapy such as working as a therapeutic drug or conjugation with siRNA, chemotherapy agents and nanoparticles.	10
2.3 Schematic representation of using AS1411 aptamer to carry ligand C8 into cancer cells overexpressing nucleolin.	12
2.4 Application of AS1411 aptamer (a) Schematic of the first- generation aptamer (RNA or DNA) -siRNA/miRNA chimera. (b) Schematic of the physical conjugation between an aptamer (DNA or RNA) and anthracycline (Dox) through intercalation.	13
2.5 Schematic illustration of the effects of miR-143 restoration on gastric cancer growth, apoptosis, and migration.	15
2.6 Structure of Dox-DNA complex.	16
2.7 The potential mechanisms of Dox-mediated cell death. Dox binds on TOP2, producing a break in the DNA chains as well as raising the reactive oxygen species (ROS).	16
4.1 Formation of MAH investigated by 10% polyacrylamide gel electrophoresis.	27
4.2 Gel electrophoresis was utilized to confirm the <i>In vitro</i> stability of MAH at day 1- day 30. Lane 6 indicates the bands for MAH, 151 bp.	28
4.3 MiR-143 expression was dramatically downregulated in Caco-2 and SW480 cells, compared to CCD841 CoN using RT-qPCR analysis.	29

4.4 Fluorescent image of (A) SW480 treated with 10 $\mu$ M FAM-labeled AS1411 aptamer, (B) SW480 treated with 10 $\mu$ M FAM-labeled NonAS1411 aptamer, and (C) SW480 without treatment.	30
4.5 Fluorescent image of (A) CCD841 CoN treated with 10 $\mu$ M FAM-labeled AS1411 aptamer, (B) CCD841 CoN treated with 10 $\mu$ M FAM-labeled NonAS1411 aptamer, and (C) CCD841 CoN without treatment.	31
4.6 MiR-143 expression was rebound in SW480 cells after treatment with MAH, $*P<0.05$ .	32
4.7 <i>KRAS</i> mRNA expression was diminished in SW480 cells after treatment with MAH, $*P<0.05$ .	33
4.8 The <i>KRAS</i> mRNA level in MAH-treated SW480 cells was comparable to one in CCD841 CoN, $*P<0.05$ .	34
4.9 Western blot analysis on SW480 cells for KRAS, AKT, and ERK was treated with MAH, MNH and untreated treatment, respectively, for 72 h, and cell lysate and was detected with antibodies against KRAS, AKT, and ERK Band intensities were quantitatively analyzed and normalized to $\alpha$ -tubulin. Data are mean $\pm$ SD from three replicates using one-way ANOVA (Dunnett's T3 test), $*P \leq 0.05$ indicates a significant difference.	35
4.10 Spectral analysis of free Dox solution fluorescence (0.95 $\mu$ M) (green line), MAH (5 $\mu$ M) (blue line), and Dox-MAH after incubation for 1.5 hours (yellow line).	36
4.11 Effect of Dox-MAH on SW480 cells proliferation. The data are shown as mean $\pm$ SD, n=3, $*P<0.05$ .	37
4.12 Effect of Dox-MAH on SW480 cells proliferation. The data are shown as mean $\pm$ SD, n=3, $*P<0.05$ .	38
4.13 Induction of apoptosis by Dox-MAH on SW480 cells analysis using flow cytometer.	39
4.14 Apoptosis-related protein alterations in SW480 cells after treatment with Dox-MAH, Dox-MNH, Dox and untreated treatment, respectively, for 72 h and cell lysate were detected with antibodies	40

against Bcl-2, Bax, and procaspase-3. Band intensities were quantitatively analyzed and normalized to  $\alpha$ -tubulin. Data are mean  $\pm$  SD from three replicates using one-way ANOVA (Dunnett's T3 test),  $*P \leq 0.05$  indicates a significant difference.



## LIST OF ABBREVIATIONS

Symbols/Abbreviations	Terms
%	Percentage
<	Less than
=	Equivalent
±	Plus-minus
α	Alpha
°C	Degree Celsius
Mg	Microgram
μL	Microliter
μM	Micromolar
A	Absorbance
ATCC	American type culture collection
CO <sub>2</sub>	Carbon dioxide
e.g.	For example
Et al.	Et alli and colleagues
g	Gram
g/mL	Gram per milliliter
i.e.	In other word
mg	Milligram
mL	Milliliter
mM	Millimolar
nm	Nanometer
OD	Optical density
rpm	Revolution per minute
SD	Standard deviation
SDS	Sodium dodecyl sulfate
SELEX	Systematic evolution of ligand by exponential enrichment
UV	Ultraviolet

## CHAPTER 1

### INTRODUCTION

According to Cancer incidence and death estimates from GLOBOCAN 2020, there were 19.3 million new cancer cases and over 10.0 million cancer-related deaths. There were 124,866 annual mortalities from cancer in Thailand and 190,636 new cases<sup>1</sup>. In 2023, an estimated 153,020 people will be diagnosed with CRC, with 52,550 deaths as a result of the disease in the United States<sup>2</sup>. CRC is the world's third most frequent cancer and the second greatest cause of cancer-related fatalities. It is the third most common cancer in men and the second most common cancer in women<sup>3,4</sup>.

According to the Hospital-based Cancer Registry 2021, the top five cancers in Thai people were colon and rectum, liver and bile duct, lung, breast, and cervical cancers. From the past to the present, cancer has been identified as the leading cause of mortality among Thai people. Also, there is a propensity to grow exponentially steadily<sup>5</sup>. Cancer is a genetic disease, indicating that it is caused by mutations in the genes that control how our body's cells behave, specifically how they proliferate and divide. KRAS mutations are observed in various malignancies and are major controlling genes. KRAS mutations are found in 50% of CRC<sup>6,7</sup>. As a result, KRAS inhibitors have significantly received research interest. KRAS is well-known to be targeted by miR-143. Therefore, a miR-143 formulation is a promising way to inhibit CRC cell growth<sup>8</sup>.

Currently available cancer therapies include surgery, radiation, chemotherapy, targeted therapy, immunotherapy, and stem cell transplants. To improve treatment efficiency, many challenging issues must be considered, such as treatment specificity, drug resistance, and undesired side effects<sup>9-11</sup>. Doxorubicin is one of several chemotherapy drugs that have severe side effects, including nausea, vomiting, diarrhea, weight loss, leucopenia, irreversible cardiotoxicity, and other conditions<sup>12, 13</sup>. These unfavorable consequences substantially limit therapy duration and drug dosage, leading to decreased therapeutic efficacy. Therefore, minimizing drug-related adverse effects is essential to enhancing chemotherapy's clinical results.

Smart Drug Delivery Systems (SDDSs) were developed to overcome these constraints by conveying molecular compounds directly to target cells. SDDS has



several potential applications and can be evolved into intelligent systems. Targeted therapy is a kind of cancer treatment that focuses on molecular targets (receptors, kinase cascades, growth factors, or molecules involved in angiogenesis and death) that are overexpressed or mutated in malignancies. Its objective is to selectively deliver chemotherapeutic drugs to cancer cells while minimizing the death of normal cells and preventing unwanted side effects<sup>14-16</sup>.

Aptamers are a class of small single-stranded DNA or RNA oligonucleotides. Aptamers are useful for a wide range of therapeutic and diagnostic applications because they may bind specifically to targets that range in size from small molecules to complex structures<sup>17,18</sup>. For example, the targeted medication delivery to cancer cells is made possible by the AS1411 aptamer, which binds to the nucleolin receptor that is overexpressed in cancer cells including CRC<sup>19,20</sup>.

MicroRNAs (miRNAs) or short non-coding RNAs (ncRNAs) are endogenous RNAs of 19-25 nucleotides in length that regulate gene expression mostly through translational inhibition or degradation of messenger RNAs (mRNA). They control the expression of genes related to cell differentiation, proliferation, and apoptosis<sup>21-23</sup>. One miRNA can have several impacts by binding to target mRNAs and regulating the translation of numerous proteins. A few studies have shown that altered expression of specific miRNAs has a role in the initiation and evolution of CRC<sup>24,25</sup>. There is also proof that, depending on the cellular environment in which they are expressed, miRNAs may function as either oncogenes or tumor suppressors. The microRNA-143 (miR-143) is known to act as a tumor suppressor, with many targets recognized in CRC such as MACC1, KLF5, KRAS, AKT, and Bcl-2<sup>23-27</sup>. When compared to its level in normal tissues, In about 80% of human colorectal tumor samples from cancer and adenoma patients, mature miR-143 expression is downregulated<sup>28</sup>. Therefore, up-regulation of miR-143 is supposed to give benefits to CRC patients because it can effectively reduce oncogene expression.

In this study, a smart drug delivery system (SDDS) was developed. It typically consists of three major components: anticancer drugs, drug carriers, and ligands on the target tumors that can be conjugated to carriers. This research aims to develop the complex composed of Dox and miR-143 as anticancer drugs, and AS1411 aptamer and hybridization strand (HBS) as drug carriers. The nucleolin receptor

targeted by AS1411 aptamer acts as a ligand on the CRC cell membrane. MiR-143, AS1411 aptamer, and HBS were combined via oligonucleotide hybridization, and subsequently loaded with Dox (Figure 1.1). Dox interacts with DNA/RNA via intercalating between the planar base pairs of duplex DNA/RNA. Dox-loaded miR143-AS1411 aptamer molecular hybrid (Dox-MAH) was tested in the CRC cells. The AS1411 aptamer worked as a signaling molecule that bound specifically to the nucleolin receptors on CRC cells, then the complex was endocytosed<sup>29</sup>, and Dox and miR-143 were released within the cells eventually (Figure 1.2). The target gene (KRAS) and its downstream genes (ERK and AKT) were downregulated leading to a reduction of cell viability and induction of apoptosis. Thus, Dox-MAH would serve as a targeted drug carrier and itself could be a potential chemotherapy drug.

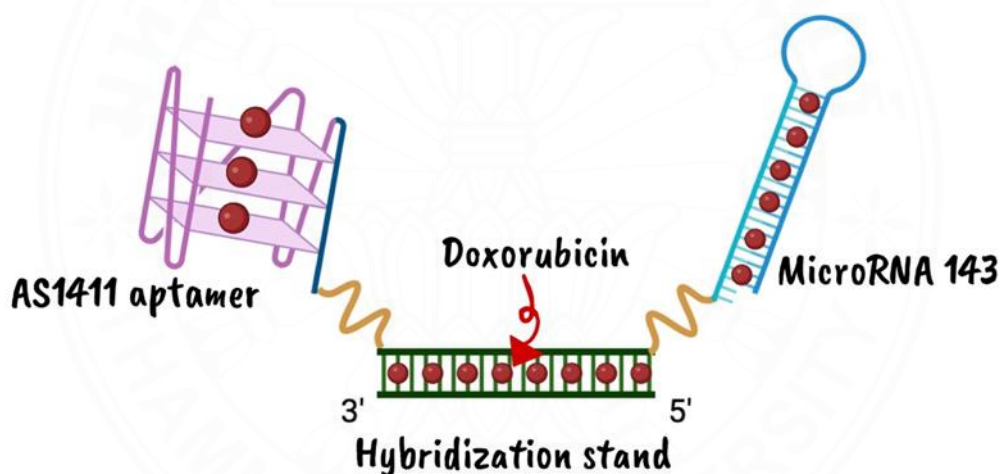


**Figure 1.1** Structure sketch of selective drug delivery systems (SDDS), Dox-Loaded Molecular Hybrid of miR-143 and AS1411 Aptamer (Dox-MAH).

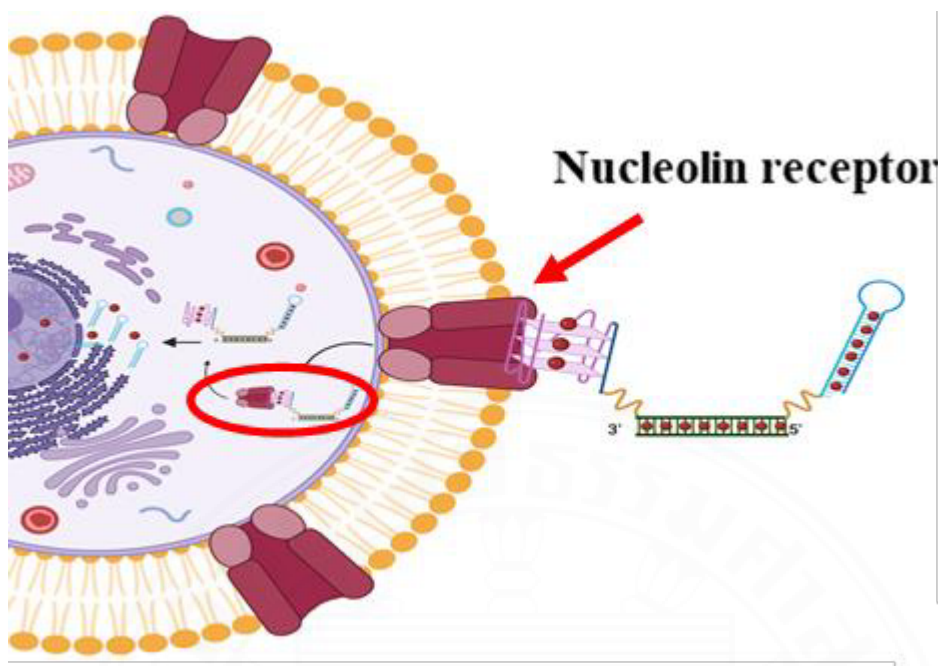


**Figure 1.2** When AS1411 aptamer binds to the nucleolin receptor on CRC cells, Dox-MAH is endocytosed, and then Dox and miR-143 are released into the cells.

### 1.1 Research Problems

In this study, we hypothesized that the simultaneous function of Dox and miR-143 can more effectively inhibit CRC cell proliferation. Also, the accurate delivery of chemotherapeutic drugs would improve the efficacy and decrease the adverse effects of chemotherapy drugs by using a selective drug delivery system (SDDS). Therefore, we proposed a strategy to prepare a molecular hybrid containing Dox, miR-143, and AS1411 aptamers. Dox-MAH was formed by oligonucleotide hybridization and Dox intercalation in the molecular hybrid. The challenges of this proposed work would focus on the successful formation of the complex, the exact delivery to target cells of Dox, and the effect of increased miR-143 level on its target genes and CRC cell growth.

## 1.2 Objective

The overall objective of this study was to prepare a Dox-loaded molecular hybrid of miR-143 and AS1411 aptamer (Dox-MAH) which can specifically bind to CRC cells, and then decrease their proliferation. Research tasks were designed as follows:

- 1) To prepare a molecular hybrid of miR-143 and AS1411 aptamer (MAH) via oligonucleotide hybridization, and intercalation containing Dox.
- 2) To test the uptake capability of AS1411 aptamer into the CRC cells by a fluorescence technique.
- 3) To evaluate the miR-143 level in CRC cells after MAH treatment.
- 4) To investigate the alteration of mRNA and protein levels of miR-143 target genes (KRAS) and its downstream target proteins (ERK and AKT) after MAH treatment.
- 5) To study the effect of Dox-MAH on CRC cell proliferation
- 6) To study the effect of Dox-MAH on the cell apoptosis pathway

## 1.3 Outcome

The finding of this research will be an alternative way to improve the treatment efficacy and hopefully decrease the adverse effects of chemotherapy drugs by using a selective drug delivery system (SDDS).

## CHAPTER 2

### REVIEW OF LITERATURE

#### 2.1 Colorectal cancer

The International Agency for Research on Cancer's GLOBOCAN 2020 projections of cancer mortality and death reported that colorectal cancer accounted for 10% of the estimated 2.3 million new cases in 2020. Lung cancer remained the leading cause of cancer death, with an estimated 1.8 million deaths (18%), followed by colorectal (9.4%), liver (8.3%), stomach (7.7%), and female breast (6.9%) cancers, which were the next most common causes <sup>1,30</sup>. According to the Hospital-based Cancer Registry 2021, CRC ranks among the top five most commonly diagnosed cancers in Thailand <sup>5</sup>.

The majority of colorectal malignancies originate as tumors on the colon or rectal lining. These growths are referred to as polyps. Cancer begins in a polyp and can spread to the colon or rectum wall over time. Cancer cells can develop into blood vessels or lymph vessels when they enter the wall. They can then spread through the bloodstream and lymphatic system to surrounding lymph nodes or distant areas of the body<sup>31</sup>. Several risk factors for CRC include being overweight or obese, not being physically active, bad nutritional habits (a diet that is high in red meats i.e., beef, pork, or liver and processed meats like hot dogs, addiction of alcoholic beverage, smoking, the progressive aging of the population and genetic. Doctors can diagnose CRC by using one or more tests such as colonoscopy, biopsy, ultrasound, x-rays, gene and protein tests, blood tests, and computed tomography (CT or CAT scan)<sup>32</sup>.

Numerous genes are associated with signaling pathways, which have been repeatedly shown to be dysregulated in CRC due to changed functions or product mutations. Several studies have identified genes involved with increased growth, invasion, progression, or apoptosis suppression in CRC cells, including RAS, EGFR, RAF, PTEN, TGFBR2, APC, SMADs, AXIN, and CTNNB1<sup>33-36</sup>. Three Ras GTPases (HRAS, KRAS and NRAS) are the most common oncogenes in human cancers.

Mutations in KRAS are present in 50% of colorectal adenocarcinoma<sup>37</sup>. KRAS proteins participate in the RAF/MEK/ERK mitogen-activated protein kinase (MAPK) signaling pathway, which is a downstream pathway of the epidermal growth factor receptor (EGFR). Mutations in the KRAS and BRAF genes cause this system to remain activated and increase tumor cell growth.<sup>38</sup>

Moreover, the regulation of these processes is significantly influenced by other molecules. For instance, chemically modified miR-143-3p expression significantly inhibits cancer cell growth in colorectal cancer cells by targeting KRAS, AKT, and ERK pathways<sup>39</sup>. Several studies have discovered that miR-143 can slow down the progression of CRC. Hong Liu et al. discovered that increased amassment of miR-143 is expected to regulate levels of KRAS protein expression, inhibiting CRC cell proliferation. The expression of miR-143 in CRC was dramatically downregulated compared with that in normal tissue<sup>8</sup>. Direct delivery of miR-143 to CRC cells improves therapeutic efficacy.

There are several mechanisms for delivering molecules or drugs to target cells. For instance, aptamer-drug conjugates for targeted drug delivery. Aptamers can be utilized to deliver specific therapeutic agents such as miRNAs and chemotherapeutic drugs<sup>40</sup>. Therapeutic medications have been delivered using a variety of aptamers designed specifically for cancer biomarkers. Many researchers have attempted to develop novel approaches and effective drug delivery systems for the treatment of CRC. Their method can improve the specificity of new drugs or molecules that are non-toxic to cancer cells. This improves treatment efficiency while decreasing toxicity to normal cells.

## 2.2 Aptamer

### 2.2.1 Overview of aptamer

Aptamers were first discovered in the 1990s as single-stranded DNA or RNA molecules having binding capacity. Aptamers are short nucleic acid sequences that have a high affinity for molecule binding, often in the 20-80 nucleotide range<sup>17, 41</sup>. Aptamer structures are composed of a variety of secondary motifs, including stem-loop, hairpin, pseudoknot, kissing loop, three-way junction, G-quadruplex, and internal bulge

structures<sup>42</sup>. Candidate binding sequences are then subjected to repetitive selection rounds, increasing the amount of high-affinity species in the library until they eventually dominate. This method is called "Systematic Evolution of Ligands by Exponential Enrichment" (SELEX)<sup>43</sup>, shown in Figure 2.1. The conventional SELEX processes usually consist of four major steps: 1. Combination: SELEX starts with an initial library of single-stranded DNA or RNA sequences that contains up to  $10^{12}$ - $10^{15}$ , and the library is subsequently combined with the target; 2. Separation: using physical or chemical means to separate the target-binding oligonucleotides; 3. Elution: separating between the library sequences that are unbound and those that are bound to the target<sup>44</sup>; 4. Amplification: The SELEX library sequences are amplified using polymerase chain reaction (PCR) to provide an enhanced library for the upcoming stage of selection. Generally, Oligonucleotide sequences with high specificity and affinity may be improved in the reservoir after 6-20 cycles, and the entire process can be tracked using traceable labels<sup>45</sup>. SELEX methodology has been significantly refined and enhanced in recent decades<sup>46</sup>.

Many innovative SELEX methods, including graphene oxide (GO)-SELEX<sup>47</sup>, cell-SELEX<sup>48</sup>, Fluorescence-activated cell sorting (FACS)-SELEX<sup>49</sup>, Photo-SELEX<sup>50</sup>, and Capture-SELEX<sup>51</sup>, have been created to simplify the technique and enhance the variety of aptamers. Aptamers are stable molecules that can withstand high temperatures and strong acid/base conditions<sup>52</sup>. Aptamers are small in size, so they may be internalized by cells and chemically modified. Furthermore, aptamers have low harm because they are nucleic acids that cannot be detected by the human immune system<sup>53</sup>.

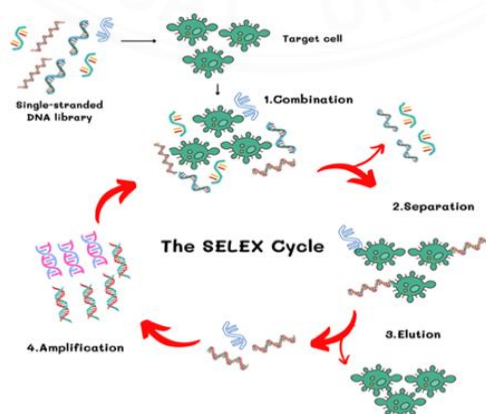


**Figure 2.1** The conventional processes of systematic evolution of ligands by exponential enrichment (SELEX).



## **2.2.2 Application of aptamer**

### **2.2.2.1 Aptamers as therapeutic agents**

Aptamers are a potential class of compounds that can be used as treatments for a variety of disorders, including various cancers and cardiovascular diseases. Aptamer oligonucleotides provide several benefits over antibodies in screening medical, bio-sensing, and bio-imaging systems due to their specificity and other unique properties such as simplicity of chemical synthesis, adjustable backbone modification, low immunogenicity, and high stability<sup>54, 55</sup>. These advantages make aptamers more widely utilized in the diagnosis and treatment of medical disorders. Aptamers are useful for detecting a variety of proteins on cell membranes or in the bloodstream and can regulate their binding with receptors, impacting the corresponding biological pathways for the treatment of various disorders, including cancer, infectious disease, and cardiovascular disease (54). Pegaptanib (Macugen®), for example, is an aptamer utilized to treat age-related macular degeneration (AMD), which has been approved by the U.S. FDA<sup>56</sup>. Pegnivacogin is used as anticoagulants. One example of an aptamer currently developed for anticancer therapy is AS1411, this is now being investigated in clinical studies for the treatment of cancer<sup>53</sup>.

### **2.2.2.2 Aptamers in the diagnosis of diseases**

Aptamers have a high affinity and specificity for binding to targets, making them suitable for use in clinical diagnostics and treatments for several diseases such as infectious disease<sup>57</sup>, hematological disease<sup>58</sup>, cardiovascular disease<sup>16</sup>, and cancer<sup>59</sup>. Toscano-Garibay et al. isolated RNA aptamers (G53N.4) with high affinity and specificity for the HPV16 E7 oncoprotein, which might be utilized to identify papillomavirus infection and cervical cancer<sup>60</sup>. Xilan Li et al. The XL-33-1 aptamer shows great promise as a molecular imaging tool for detecting lymph node tissue linked with colon cancer metastases early on<sup>61</sup>.

### **2.2.2.3 Aptamer-drug conjugates (ApDCs) for targeted drug delivery**

Not only do they function as therapies by themselves, but aptamers have also been thoroughly investigated as ligand targets for ApDC drug delivery. The FDA has previously authorized several of these for cancer therapy. Aptamer ligands, drug moieties, and linkers bridging the aptamers and drug moieties



are the three components of typical ApDCs. ApDCs have been investigated for a variety of therapeutic approaches, including chemotherapy, small interfering RNAs (siRNAs), microRNAs, immunotherapy, and nanoparticles<sup>55, 62, 63</sup> (Figure 2.2).

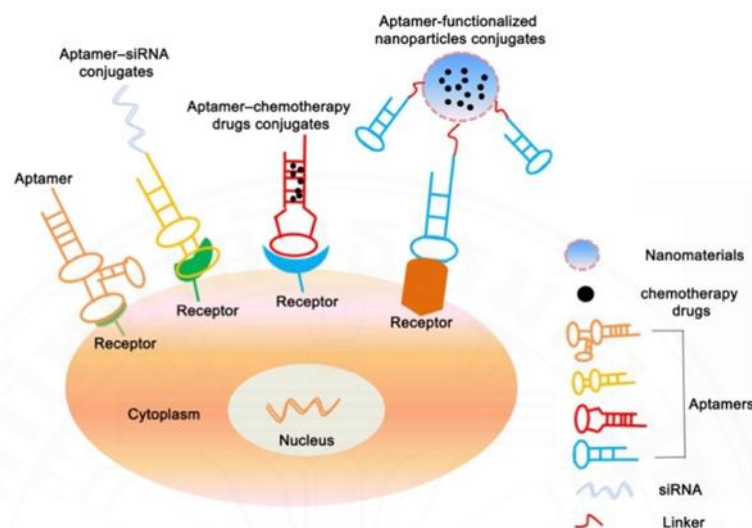


**Figure 2.2** Applications of aptamers in cancer therapy such as working as a therapeutic drug or conjugation with siRNA, chemotherapy agents and nanoparticles<sup>63</sup>

#### 2.2.2.4 ApDCs for chemotherapy

One of the most often utilized methods of treating cancer is chemotherapy. The toxicity of chemotherapeutic drugs in healthy tissues and the unwanted side effects that affect overall treatment effectiveness are typical restrictions. Reducing the accessibility of these medications to healthy tissues could thereby lessen these negative effects and increase therapeutic effectiveness. Consequently, research has been done on aptamer-mediated targeted drug delivery, which delivers medications to diseased tissues or cells but not to healthy tissues<sup>64</sup>. Additionally, aptamers and medications can be covalently conjugated to create ApDCs. For example, the chemotherapeutic drug DOX can interact with double-stranded DNA<sup>65</sup>. As an example, Huang et al. designed and synthesized a sgc8-Dox conjugate that specifically kills the target CCRF-CEM cell for the treatment of acute myeloid leukemia (AML)<sup>66</sup>. Rotkrue et al. used a Dox-loaded Chol-aptamer molecular hybrid (Dox-CAH) to specifically kill CRC with no significant off-target side effects<sup>29</sup>.

### **2.2.2.5 ApDCs for gene therapy**

Treating illnesses by the correction of corresponding genetic defects is a promising strategy known as gene therapy. Gene therapy approaches can be implemented at the genome or transcriptome level. Using RNA interference (RNAi), microRNAs and antisense oligonucleotide technologies, mRNA functions can be suppressed in transcriptome approaches. Gene therapy, like many other therapeutic treatments, lacks specificity for diseased cells, which makes it critical to successfully deliver the gene therapy agents. Aptamers might be helpful to selectively deliver gene therapeutics into diseased cells<sup>64</sup>. For example, MUC1 aptamer conjugated with microRNA-29b for the treatment of ovarian cancer<sup>67</sup>. By targeting and inhibiting Axl, the aptamer-GL21.T-miRNA-34c combination may diminish non-small cell lung cancer cell growth, circumventing RTK inhibitor resistance<sup>68</sup>.

### **2.2.3 AS1411 aptamer**

#### **2.2.3.1 Overall of AS1411 aptamer**

AS1411, formerly named ARGO100, is a 26-nucleotide guanosine-rich DNA aptamer, formed as a G-quadruplet. AS1411 has a high affinity to nucleolin, a protein that is frequently overexpressed or translocated on the surface of cancer cells<sup>69</sup>. As the first oligodeoxynucleotide aptamer to be studied in phase I and II clinical trials for the treatment of cancers, including, prostatic<sup>70</sup>, colorectal<sup>29</sup>, breast cancer<sup>71</sup>, and acute myelogenous leukemia (AML), AS1411 was developed by Antisoma PLC.<sup>72</sup>, , and. AS1411 has an anti-proliferative effect on cancer cells<sup>73</sup>. It can up-regulate p53 and down-regulate Bcl-2 and Akt1 through modulating nucleolin, leading to the inhibition of cell migration<sup>71, 73</sup>. Nucleolin is a multifunctional nucleolar phosphoprotein, having a molecular weight of 100 kDa, which is highly expressed in growing eukaryotic cells. Nucleolin is an RNA-binding protein (RBP) that controls cell proliferation and growth such as cytokinesis, replication, embryogenesis, and nucleogenesis<sup>74</sup>. Furthermore, since nucleolin is extensively expressed on the surface of several tumor cells, it might regulate tumors' specific reception of specific molecular receptors<sup>75</sup>.

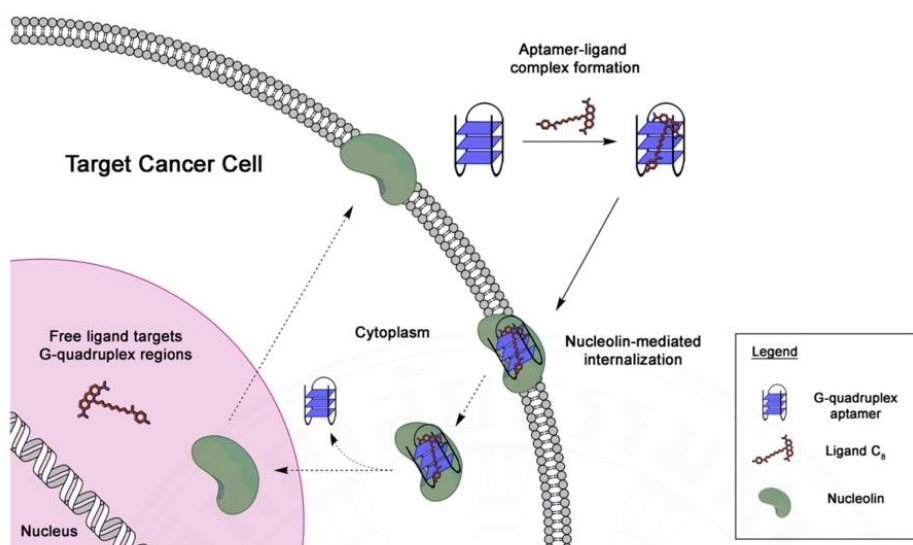


**Figure 2.3** Schematic representation of using AS1411 aptamer to carry ligand C8 into cancer cells overexpressing nucleolin.<sup>76</sup>

### 2.2.3.2 Application of AS1411 aptamer in cancer

The first aptamer being tested in clinical trials for the treatment of cancer in humans is AS1411. AS1411 has an anti-proliferate effect on several cancer cells<sup>29, 70-73</sup>. It was developed for specific drug delivery to tumors by conjugating with several materials such as RNA interference (RNAi), which is a novel class of therapies being developed to treat human diseases such as pancreatic cancer, liver cancer, CRC, advanced solid tumor, respiratory syncytial virus, hepatitis B virus, and HIV-1<sup>77, 78</sup>. The drug cisplatin-resistant ovarian cancer was designed to be treated with AS1411 aptamer-PEGylated PLGA that contains anti-miRNA-21 and cisplatin<sup>79</sup>. Furthermore, AS1411 was combined with chemotherapeutic drugs by using Dox's ability to intercalate inside nucleic acid helical strands (Figure 2.4)<sup>80</sup>. Trinh et al. used formaldehyde as a crosslinking agent to conjugate AS1411 with Dox. Dox could be delivered to liver cancer cells (Huh7 cells) just as effectively by the AS1411-Dox complex and with the same efficiency as free Dox did. AS1411-Dox inhibited Huh7 tumor development with approximately equal activities to independent Dox<sup>81</sup>

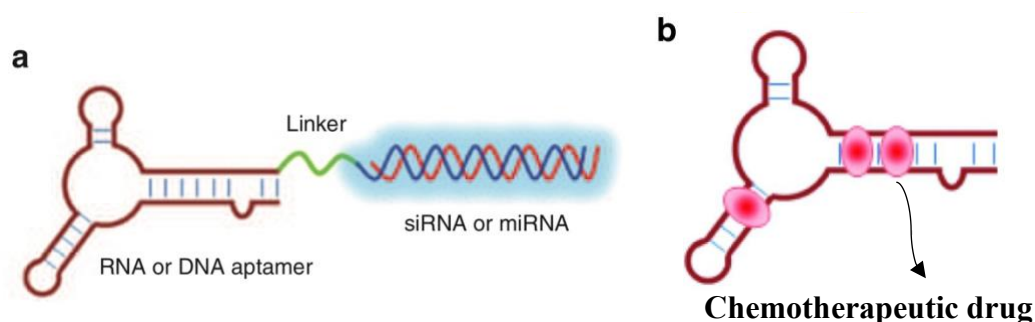


**Figure 2.4** Application of AS1411 aptamer (a) Schematic of aptamer (RNA or DNA) link with siRNA/miRNA. (b) Schematic of the physical conjugation of an aptamer (DNA or RNA) with an anthracycline medication (Dox) through intercalation<sup>80</sup>

## 2.3 MicroRNAs

The mechanism by which microRNAs (miRs), a type of extremely short non-coding RNAs (18–22 nucleotides), work is to match base pairs in their seed sequences (nucleotides 2–7) with the 3' untranslated regions (3'UTR) of target RNA<sup>82</sup>. Mature miRNAs are integrated into the RNA-induced silencing complex (RISC) and bind to 3'UTRs of particular target mRNAs to limit translation and occasionally induce mRNA degradation<sup>83</sup>. Since the discovery of miRNAs in *Caenorhabditis elegans* in 1993<sup>84, 85</sup>, many miRNAs have been found in metazoans, plants, viruses, and eukaryotes, including humans<sup>86, 87</sup>. It is predicted that at least 30% of protein-coding genes are regulated by miRNAs, which make about 1%–5% of the human genome<sup>88, 89</sup>. MiRNAs are also involved in important processes such as developmental time regulation, hematopoietic cell differentiation, apoptosis, cell proliferation, and organ development<sup>90, 91</sup>.

### 2.3.1 MicroRNAs in cancer

The multi-step process of cancer involves genetic changes in normal cells that lead from pre-malignant phases (initiation) to invasive cancer (progression) that can spread everywhere the body (metastasis). Growth signals are not necessary for cancer cells to multiply; they may also be resistant to inhibitory growth signals, avoid intrinsic cell replication limitations, elude programmed cell death (apoptosis) pathways, promote and maintain angiogenesis, and proliferate into new colonies apart from the

primary tumor<sup>92</sup>. Cancer development and progression are linked to the deregulation of genes involved in cell proliferation, differentiation, and/or death. Oncogenes and tumor suppressors are two types of genes that are associated with cancer formation<sup>93</sup>. Genetic modifications that boost the gene can activate oncogenes, change promoters/enhancers to increase gene expression, or change protein structure to a permanent active state<sup>93-95</sup>. In contrast, tumor suppressor gene products regulate biological processes. Dysfunction of tumor suppressors occurs from the loss or decline of function<sup>96</sup>. Most cancers have been shown to have dysregulated miRNA expression patterns<sup>97</sup>. Furthermore, the expression of miRNAs can decide whether they act as oncogenes or tumor suppressors in a specific cell environment<sup>98, 99</sup>.

### 2.3.2 MicroRNA-143

MiR-143 is a tumor suppressor miRNA that is downregulated in a variety of human cancers<sup>99, 100</sup>. This miRNA has a preventive function in tumor growth and influencing the expression of various genes, including KRAS, BCL2, ERK5, C-Myc, Bax, caspase-3, caspase-9, and ELK1 that are associated with cell growth, survival, differentiation, and invasion<sup>25, 100-103</sup>. In contrast to normal tissues, mature miR-143 expression was consistently downregulated in approximately 80 percent of human colorectal tumor samples from cancer and adenoma patients<sup>28</sup>. According to research, miR-143 downregulation is linked to cancer growth, apoptosis, and metastasis<sup>104, 105</sup>. These occurrences might be potentially due to the lack of regulatory effects of miR-143 on the previously indicated genes. KRAS is an important signaling molecule in viable cells. KRAS mutations play a critical role in the growth of malignant cells. Furthermore, the C-Myc transcription factor is a critical regulator of cell proliferation and has therapeutic relevance in a variety of cancers, including lung, pancreatic, and colorectal tumors<sup>103, 106</sup>. Enhanced miR-143 accumulation is likely to influence the KRAS protein production at the post-transcriptional stage by interacting selectively with the complementary site, hence decreasing CRC cell proliferation<sup>8</sup>. Restoring miR-143 expression reduced proliferation and migration in the MKN-45 gastric cancer cell line, as well as decreased expression of potential miR-143 targets KRAS, MMP9, and C-Myc. Furthermore, as shown in figure 2.5, miR-143 expression can trigger apoptosis in MKN-45 cells by raising the expression of Bax, caspase-3, and caspase-9<sup>106</sup>.

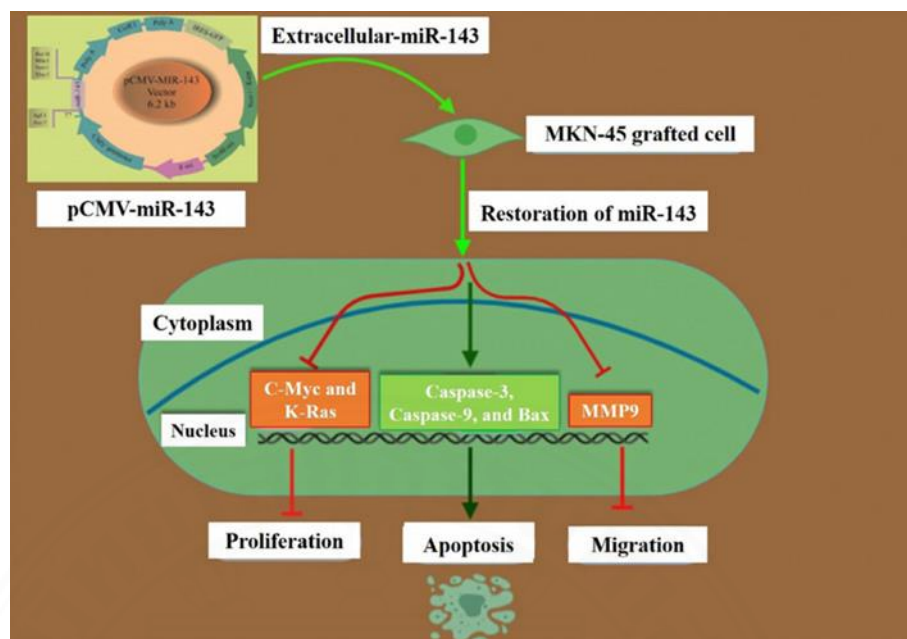


**Figure 2.5** Schematic illustration of the effects of miR-143 restoration on gastric cancer growth, apoptosis, and migration<sup>106</sup>.

## 2.4 Doxorubicin

Doxorubicin (Dox), commonly called Adriamycin in the pharmaceutical industry, is a chemotherapy medication that is utilized to treat various types of solid tumors, including breast<sup>107</sup>, lung<sup>108</sup>, ovarian<sup>109</sup>, and bladder cancer<sup>110</sup>, Kaposi's sarcoma<sup>111</sup> and multiple myeloma, acute leukemia, and lymphoma are examples of hematological malignancies<sup>112</sup>. In the 1960s, the bacterium *Streptomyces peucetius* was utilized for the first time to produce DOX<sup>113</sup>. Dox belongs to the anthracycline and antitumor antibiotic family<sup>114</sup>. Dox's cytotoxic effect is complex, involving DNA intercalation (Figure 2.6), suppression of DNA topoisomerase II, inhibition of RNA and DNA polymerases, strand breakage, and the production of free radicals<sup>13, 115</sup>. Dox can intercalate into genetic material mostly at GC-rich sites, inhibiting the advancement of topoisomerase II, an enzyme that relaxes supercoils in DNA to allow replication and transcription<sup>116</sup>. After establishing the Dox-topoisomerase-II complex, it has broken the DNA chain for replication, blocking the release of the DNA double helix and therefore ending the replication process<sup>117</sup>. It may also enhance the formation of quinone, a type



of free radicals, which can lead to cytotoxicity<sup>118</sup>. Dox, by intercalation, can also cause histone eviction from transcriptionally active chromatin<sup>116, 119, 120</sup>. As shown in figure 2.7, Dox-exposed cells exhibited dysregulations of DNA damage response, epigenome, and transcriptome<sup>118</sup>.

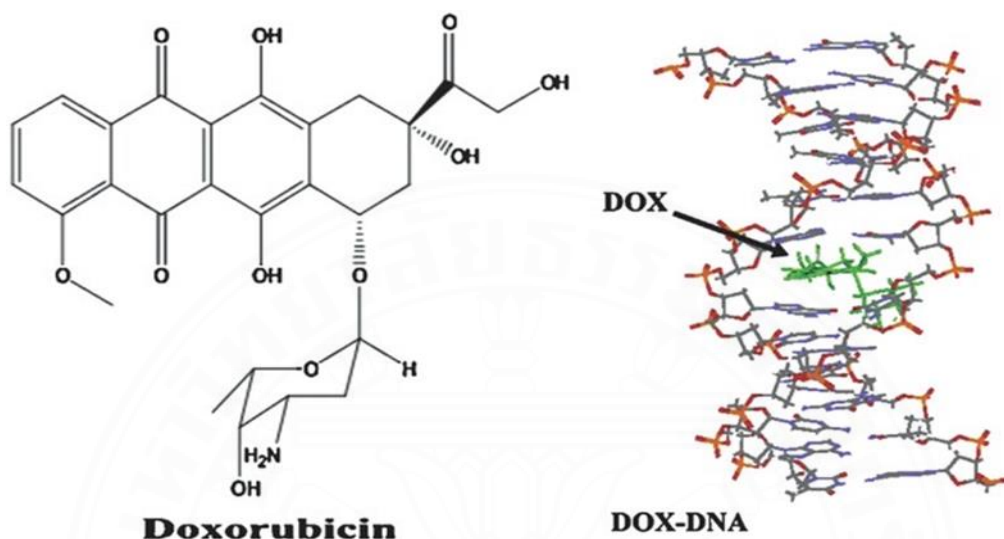


**Figure 2.6** Structure of Dox-DNA complex<sup>120</sup>.

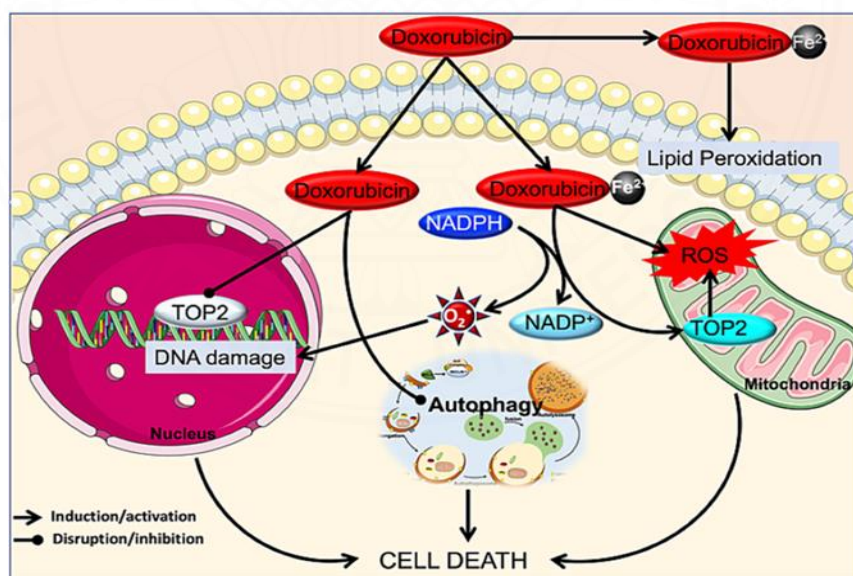


**Figure 2.7** The potential mechanisms of Dox-mediated cell death. Dox binds on TOP2, producing a break in the DNA chains as well as raising the reactive oxygen species (ROS)<sup>118</sup>.

Although Dox has been used for decades and its efficacy and safety have been well established, side effects include bone marrow suppression (i.e., immunosuppression), cardiotoxicity, nausea, vomiting, diarrhea, hemorrhagic cystitis, baldness, rash and inflammation of the mouth, unusual bleeding or bruising, and crimson urine have been reported<sup>114, 121</sup>. To maximize therapy efficiency and avoid adverse effects, Dox doses for specific tumors must be evaluated. Targeted drug delivery to cancer cells is a potential strategy for reducing adverse effects. Also, coupling Dox with another medication can reduce its toxicity<sup>122</sup>. Dox can be used in conjunction with other molecules such as liposomes, microRNAs, and aptamers<sup>123-125</sup>.





## CHAPTER 3

### RESEARCH METHODOLOGY

#### 3.1 Chemicals and reagents

30% Acrylamide solution	(Bio-Rad, USA)
Ammonium persulfate, (APS)	(Calbiochem®, USA)
4',6-diamidino-2-phenylindole (DAPI)	(Sigma-Aldrich, USA)
Dimethyl sulfoxide, (DMSO)	(Sigma-Aldrich, USA)
Doxorubicin hydrochloride (DOX)	(Fresenius Kabi, Thailand)
Dulbecco's Modified Eagle Medium, (DMEM)	(Gibco, USA)
Fetal bovine serum, (FBS)	(Gibco, USA)
3-(4, 5-dimethylthiazol-2-yl-5-(3-carboxymethoxyphenyl)-2-(4-sulfophenyl)-2H-tetrazolium (MTS) solution	(Promega, USA)
Penicillin-streptomycin, (Pen/Strep)	(Gibco, USA)
Phosphate-buffered saline, (PBS)	(Bio Basic, Canada)
Polyacrylamide solution (30%)	(Bio-rad, USA)
Sodium bicarbonate, (NaHCO <sub>3</sub> )	(BHD, England)
Sodium dodecyl sulfate, (SDS)	(Calbiochem®, USA)
N,N,N,N'-tetramethylethylenediamine, (TEMED)	(Calbiochem®, USA)
Trypsin-EDTA	(Gibco, USA)
Tris-base	(Bio-Rad, USA)
TRIzol reagent	(Thermo Scientific, USA)
TaqMan® MicroRNA Reverse Transcription Kit	(Thermo Scientific, USA)
TaqMan® 2x Universal PCR Master Mix,	(Thermo Scientific, USA)
No AmpErase® UNGb	
U6	(Thermo Scientific, USA)
Hsa-miR-143	(Thermo Scientific, USA)

### 3.2 Instruments and lab equipment

25, 75 cm <sup>2</sup> plastic tissue culture flasks	(Costar Corning, USA)
12, 24, 96-well plate	(Costar Corning, USA)
Autoclave	(Hirama, Japan)
Autopipette	(Rainin, USA)
Biosafety cabinet	(Faster srl, Italy)
Centrifuge machine	(Hettich, Germany)
200 µL Centrifuge tube	(Costar Corning, USA)
1, 15, 50 mL centrifuge tube	(Costar Corning, USA)
CO <sub>2</sub> incubator	(Shel lab, USA)
5, 10, 25, 50 mL disposable pipette	(Costar Corning, USA)
Electrophoresis set	(Bio-Rad, USA)
Flow cytometer	(BD Biosciences, USA)
Refrigerator	(Sanyo, Japan)
-20 °C Freezer	(Sanyo, Japan)
-80 °C Freezer	(Thermo Scientific, USA)
Glass bottles	(Duran, Germany)
Glassware	(Duran, Germany)
Hemocytometer	(Boeco, Germany)
Hot air oven	(Mettler, Germany)
Hotplate	(Stuart, UK)
Inverted microscope	(Nikon, USA)
Laminar air flow cabinet	(Bosstech, USA)
Liquid nitrogen tank	(Taylor-Wharton, USA)
Magnetic stirrer	(Ika Werke, Germany)
0.5-10 µL micropipettes	(Gilson, USA)
1-20 µL micropipettes	(Gilson, USA)
20-200 µL micropipettes	(Gilson, USA)
100-1000 µL micropipettes	(Gilson, USA)
Microplate spectrophotometer	(Thermo Scientific, USA)
Mini-Gel electrophoresis unit	(Bio-Rad, USA)

Gel doc	(Bio-Rad, USA)
Applied Biosystems StepOne™/ StepOnePlus™	
Real-Time PCR System	(Thermo Scientific, USA)
Mastercycler nexus Gradient	(Eppendorf, Germany)
pH meter	(Thermo Scientific, USA)
Pipette tips	(Kirgen, USA)
Pipette controller	(Brand, Germany)
Power supply	(Bio-Rad, USA)
Quick spin	(Extra Gene, Taiwan)
Refrigerated centrifuge	(Beckman coulter, USA)
Vortex mixer	(Scientific Industries, USA)
UV Lamp	(Scientific industries, USA)
UV-VIS spectrophotometer	(Shimadza, Japan)
Water bath	(Mettler, Germany)

### 3.3 Sequence design for miR-143, AS1411 aptamers, and a hybridization strand

To provide the hybridization site for AS1411 aptamer and miR-143, additional oligonucleotides completely compatible with a hybridization strand were added to the original sequence of AS1411 and miR-143 at 5'end. Meanwhile, A hybridization strand, which is a sequence, was created to complement those additional areas (Figure 1.1).

The miR-143 was modified with a 2'-O-Methylation (2'OMe) to make it more stable and to prevent it from degradation before entering the cell. The hybridization of these sequences was pre-studied by an OligoAnalyzer™ tool developed by the oligonucleotide supplier (IDT, USA).

### **3.4 Formation of molecular hybrid of miR-143 and AS1411 aptamer (MAH)**

MiR-143, AS1411 aptamer, and hybridization strand were combined at a final concentration of 1  $\mu$ M. The mixture was then incubated at room temperature for 48 hours to allow to produce MAH by intermolecular hybridization. The hybridization result was validated using 10% native polyacrylamide gel electrophoresis.

### **3.5 *In vitro* stability of MAH**

MiR-143, AS1411 aptamer, and a hybridization strand were mixed at a final concentration of 1  $\mu$ M in Dulbecco's modified Eagle's medium (DMEM) at 37°C, 5% CO<sub>2</sub> atmosphere for 1-7, and 30 days, allowing the formation of MAH. The stability of MAH was examined by 10% native polyacrylamide gel electrophoresis.

### **3.6 Cell culture**

A human colorectal adenocarcinoma cell line (SW480 and Caco-2) and a normal colon epithelial cell line (CCD 841 CoN) were obtained from American Type Culture Collection (ATCC, USA). The cells were cultured in Dulbecco's modified Eagle's medium (DMEM) (Gibco, USA), containing 10% fetal bovine serum (FBS) (Gibco, USA) and 1% penicillin-streptomycin (Gibco, USA) at 37°C, 5% CO<sub>2</sub> atmosphere. After reaching 80% confluence, the cells were subcultured with 0.05% trypsin in phosphate-buffered saline (PBS).

### **3.7 Quantification of endogenous miR-143 in CRC and normal colon cell lines using RT-qPCR**

Total RNA was extracted from the three types of cultured cells (SW480, Caco-2, and CCD 841 CoN) using miRNeasy Micro Kit (Qiagen, USA) according to the manufacturer's guidelines. The mature miR-143 was assessed using TaqMan microRNA Assays (Applied Biosystems, USA) with the Mastercycler nexus Gradient (Eppendorf, Germany). Briefly, 10  $\mu$ g total RNA was reverse-transcribed to cDNA

using a TaqMan<sup>TM</sup> microRNA reverse transcription kit (Applied Biosystems, USA), and the expression of miR-143 was evaluated by qPCR. The primer sequences (Applied Biosystems, USA) were as follows, human U6 forward primer: 5'-CGCTTCACGAATTTGCGTGTC-3' and human U6 reverse primer: 5'-GCTTCGGCAGCACATATACTAAAAT-3'. The U6 small nuclear RNA was used for normalization of miRNA, and the relative expression level of miR-143 was calculated by the  $2^{-\Delta\Delta C_t}$  method.

### **3.8 *In vitro* cellular uptake of MAH**

#### **3.8.1 Study of AS1411 binding capability using a fluorescence microscope**

SW480 and CCD841 CoN cells ( $3 \times 10^4$  cells) were added into each well of the 96-well plates and incubated overnight at 37 °C, 5% CO<sub>2</sub> atmosphere. Subsequently, the medium was eliminated, and the cells were then treated with an MAH and a complex of miR-143+Non-specific aptamer + HBS (MNH) at concentrations of 10 μM in a final volume of 100 μL DMEM for 1 hour, and non-treated cells served as a control. Then, nuclei were stained with 100 μL of 4', 6'-diamidino-2- phenyl indole dihydrochloride (DAPI) solution (Sigma-Aldrich, USA) for 10 minutes. After that, cells were washed with PBS. Finally, ECLIPSE Ts2R inverted fluorescent microscope (Nikon, USA) was used for cell observation and imaging. The binding ability of MAH and MNH to SW480 cells and CCD 841 CoN was then examined. For microscopic visualization, green-emitting fluorescein (FAM) was linked to AS1411 aptamer and Non-specific aptamer.

#### **3.8.2 RT-qPCR analysis of exogenous miR-143**

SW480 cells ( $1 \times 10^5$ ) were put to each well of 24-well plates and incubated overnight at 37 °C, 5% CO<sub>2</sub> atmosphere. After removing the medium, the cells were treated with 10 μM MAH and MNH in 400 μL DMEM for 48 hours at 37 °C, 5% CO<sub>2</sub> atmosphere. Non-treated cells were used as a reference. Cells were washed twice with 500 μL PBS, then treated with 200 μL of 0.05% trypsin-EDTA and incubated for 5 minutes at 37 °C, 5% CO<sub>2</sub> atmosphere. After adding 400 μL of DMEM, the mixture was transferred to a 1.5 mL tube and centrifuged for 5 minutes at 1000 rpm. The cells

were washed twice with 500  $\mu$ L PBS and extracted total RNA using the previously stated procedure.

### **3.9 Investigation of alteration of miR-143 target gene products**

#### **3.9.1 RT-qPCR analysis of *KRAS* mRNA**

Total RNA was extracted 48 hours after MAH and MNH transfection using the previously described procedure. Using a High Capacity cDNA Reverse Transcription Kit (Applied Biosystems, USA), ten  $\mu$ g of total RNA was reverse transcribed into cDNA. The reaction temperature was 25 °C for 10 min, 37 °C for 120 min, and 85 °C for 5 minutes. Real-time PCR was used to quantify the quantity of *KRAS* and *GAPDH* transcripts using TaqMan Gene Expression Assays with FAM-conjugated MGB (minor groove binder) probes for *KRAS* (cat# Hs00364282\_m1) and *GAPDH* (cat# Hs99999905\_m1). The reactions were incubated at 95 °C for 10 minutes, followed by 40 cycles at 95 °C for 15 seconds and 60 °C for 60 seconds. A real-time PCR was carried out by StepONEplus, and the results were analyzed with the comparative delta Ct method, using the Step ONEplus analysis software.

#### **3.9.2 Western blot analysis of *KRAS*, ERK, and AKT proteins**

After 72 hours, the MAH and MNH-treated SW480 cells were collected. The cell pellets underwent three rounds of cold PBS washing before being lysed using RIPA buffer (Amersco, USA) that contained protease inhibitors. The cells were then sonicated until all of the liquid was removed. A Pierce BCA protein assay kit (Thermo Scientific, USA) was used to quantify the amount of protein. Polyacrylamide gel electrophoresis (PAGE, 12% resolving gel and 4% stacking gel) was used to separate the cell lysates, which were then transferred to a PVDF membrane using electrical blotting. After blocking with Odyssey blocking solution for one hour at room temperature. The membranes were treated with *KRAS*, ERK, AKT, and  $\alpha$ -tubulin (internal control) primary antibody (K-Ras Recombinant Rabbit Monoclonal Antibody (11H35L14) Cat #703345 (Thermo Scientific, USA), p44/42 MAPK (Erk1/2) Antibody Cat #9102, Akt Antibody Cat #9272, polyclonal anti- $\alpha$ -tubulin Cat # 2144) (Cell Signaling Technology, USA) at 4 °C overnight. The membranes were then treated with

the secondary antibody at room temperature for an hour. The LI-COR Odyssey Imager (LI-COR, USA) was used for band visualization and quantification.

### 3.10 Intercalation of Dox into MAH

The production of DOX-MAH molecules depends on the effectiveness of Dox intercalation into the CG site of oligonucleotide duplexes. After 1.5 hours at room temperature, 5  $\mu\text{M}$  of MAH and 0.95  $\mu\text{M}$  of Dox were combined in phosphate-buffered saline (PBS, pH 7.4). After then, the fluorescence spectra of Dox and Dox-MAH were measured with a Varioskan LUX microplate reader (Thermo Scientific, USA) ( $\lambda_{\text{Em}}$  = 500-800 nm,  $\lambda_{\text{Ex}}$  = 480 nm).

### 3.11 CRC and normal colon cell proliferation assay after Dox-MAH treatment

To investigate the impact of MAH on the proliferation of colon cancer and normal colon cells,  $5 \times 10^3$  cells/well of SW480 and CCD 841 CoN cells were seeded into 96-well plates using DMEM. The cells were then incubated for 24 hours at 37°C with 5% CO<sub>2</sub> atmosphere. Following the removal of the medium, the cells were treated with MAH, MNH, Dox, Dox-MAH, and Dox-MNH at 10  $\mu\text{M}$  complex and 0.95  $\mu\text{M}$  Dox in 100  $\mu\text{L}$  DMEM. As a control, untreated cells were used. To evaluate cell viability, 20  $\mu\text{L}$  of MTS solution (Promega, USA) was added to each well and incubated at 37°C for 1 hour. Finally, the absorbance was measured at 490 nm using a Multiskan FC microplate reader (Thermo Scientific, USA). The percentage of cell viability was calculated by the following equation: Percentage of cell viability =  $(A_{\text{test}} - A_{\text{blank}}) / (A_{\text{control}} - A_{\text{blank}}) \times 100\%$ <sup>126</sup>.  $A_{\text{test}}$  is the absorbance of the treated cells,  $A_{\text{control}}$  is the absorbance of untreated cells, and  $A_{\text{blank}}$  is the absorbance of the MTS solution without cells.

### 3.12 Detection of CRC cell apoptosis after Dox-MAH treatment

The cells were cultivated and treated with Dox, Dox-MAH, and Dox-MNH following the same methodology as described previously. Following treatment, the cells were washed twice with PBS, treated for 15 minutes with FITC Annexin V/propidium iodide (PI) apoptosis detection reagent, and further investigated using a flow cytometer. Apoptotic cells were identified by labeling phosphatidylserine molecules that had translocated to the outside of the cell membrane with FITC Annexin V. The PI tagged the cellular DNA in late apoptotic and necrotic cells whose membranes had been damaged.

### 3.13 Western blot analysis of procaspase-3, Bax and Bcl-2 proteins in the apoptosis pathway

SW480 cells were treated with 0.95  $\mu$ M Dox, 5  $\mu$ M Dox-MAH, and 5  $\mu$ M Dox-MNH for 72 hours. After that, cells were collected and performed the western blot analysis using the described protocol with the relevant primary antibodies such as procaspase-3, Bax, BCL2 and  $\alpha$ -tubulin (internal control) (Caspase-3 Antibody Cat #9662, Bax Antibody Cat #2772, Bcl-2 (D55G8) Rabbit mAb Cat #4223, polyclonal anti- $\alpha$ -tubulin Cat# 2144) (Cell Signaling Technology, USA).

### 3.14 Statistical analysis

All data were represented as the mean  $\pm$  standard deviation (SD) of at least triplicate samples. A comparison between the control and study groups was performed by one-way analysis of variance (ANOVA) followed by Dunnett's T3 test. Statistical significance was defined as \*  $P < 0.05$ .



## CHAPTER 4

### RESULTS AND DISCUSSION

#### 4.1 Sequence design for aptamers, miR-143, and a hybridization strand

To establish a hybridization site for the AS1411 aptamer and miR-143, additional oligonucleotides completely compatible with the hybridization strand (HBS) were extended at the 5' end. Furthermore, hybridization strands were designed to complement those specific regions. miR-143 was modified with a 2'-O-Methylation (2'OMe) in two positions: in the naturally modified position and the 3' end position<sup>127</sup>, to make it more stable and to prevent it from degrading before entering the cell. The sequence of HBS was complementary to the additional oligonucleotides of the aptamer and miR-143. Hybridization between these sequences was tested using the Oligo Analyzer tool (IDT, USA), and the sequences were summarized in Table 4.1.

**Table 4.1** List of oligonucleotides and their modification

Name	Modification	Sequence 5' → 3'
miR-143	2'-O-Methylation	5'- <u>UGAGAUGAAGCA</u> <u>CUGUAGCUC</u> CCTGACTTGAGCAAAATTGACT-3'
As1411 aptamer		5'- <u>GGTGGTGGTGGTTGTGGTGGTGGTGG</u> CCATCGGCTATCGAAGCTCGAT-3'
Non-specific aptamer		5'- <u>TTCCTCCTCCTCCTTCTCCTCCTCCTCC</u> ATCGGCTATCGAAGCTCGAT-3'
Hybridization stand (HBS)		5'-TCCAGTTTTTAAGTCAATTTTGCTCAAGTCAC ACCCCGCTAATCGAGCTTCGATAGCCGAT-3'

The original sequences of miR-143, AS1411 aptamer, and Non-specific aptamer were indicated by underlining, and the modified bases were highlighted in red.

## 4.2 Formation of molecular hybrid of miR-143 and AS1411 aptamer (MAH)

In order to produce MAH, a combination of the aptamer, miR-143, and HBS at room temperature for 48 hours. Then, the products were examined by 10% native polyacrylamide gel electrophoresis. There was a partitioned band corresponding to the size of MAH (Figure 4.1, Lane 6). MAH was successfully formed via intermolecular hybridization of those oligonucleotide sequencing.

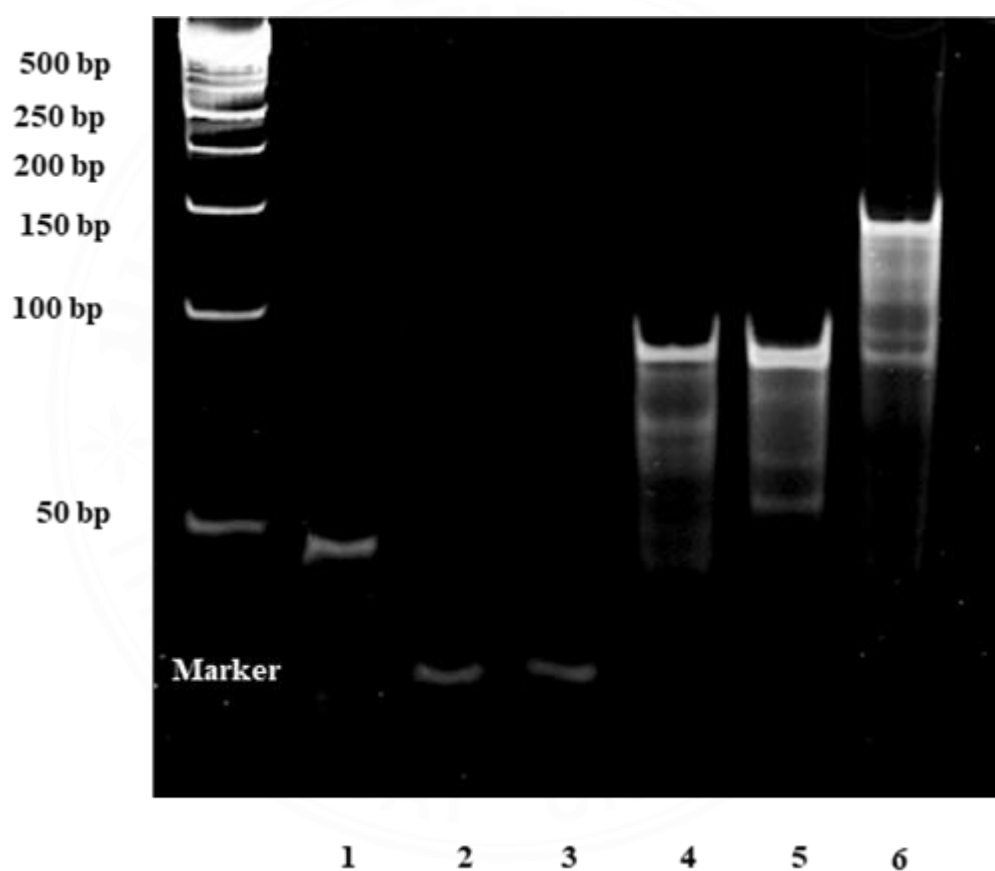


**Figure 4.1** Formation of MAH investigated by 10% polyacrylamide gel electrophoresis. (Lane 1 HBS =60bp, Lane 2 AS1411 aptamer =48bp, Lane 3 miR-143 =43bp, Lane 4 HBS+AS1411 aptamer =108bp, Lane 5 HBS+miR-143 =103bp and Lane 6 HBS+AS1411 aptamer+miR-143 or MAH =151bp)

### 4.3 *In vitro* stability of MAH

In order to create MAH, a combination of the aptamer, miR-143, and HBS in DMEM at 37°C, 5% CO<sub>2</sub> atmosphere for 1-7, and 30 days. Then the products were examined by 10% native polyacrylamide gel electrophoresis. When examining the findings from day 1 to day 7 and day 30, the results showed that MAH (lane 6) was extremely stable (Figure 4.2). The bands were still visible at even day 30, and the amount of MAH had slightly increased with time from day 1 to day 7, indicating longer incubation time might result in a larger number of products. Although miR-143 (lane 3) had a 2'-O-methyl group that shielded them from exonucleolytic 3'-to-5' activity and made them more stable<sup>127</sup>, miR-143 was less stable and more easily demolished than DNA<sup>128</sup>.

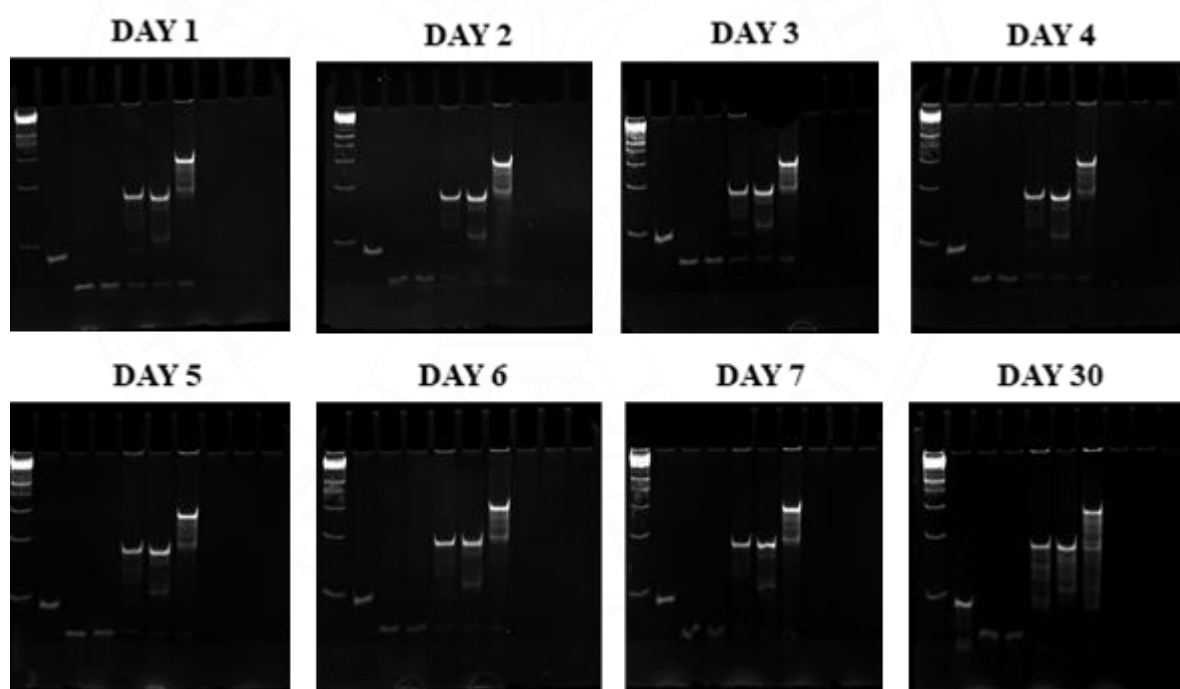


**Figure 4.2** Gel electrophoresis was utilized to confirm the *In vitro* stability of MAH at day 1 – day 30. Lane 6 indicates the bands for MAH, 151 bp.

#### 4.4 Quantification of endogenous miR-143 in CRC and normal colon cell lines using quantitative reverse transcription polymerase chain reaction (RT-qPCR)

We initially investigated miR-143 expression levels in two human colorectal cancer cell lines (SW480 and Caco-2) as well as a normal colon epithelial cell line (CCD 841 CoN). When compared to normal cells, miR-143 expression levels were downregulated in both SW480 and Caco-2. However, the amount of miR-143 in SW480 was significantly lower than in Caco-2 (Figure 4.3). As a result, SW480 cells were selected for further investigation.

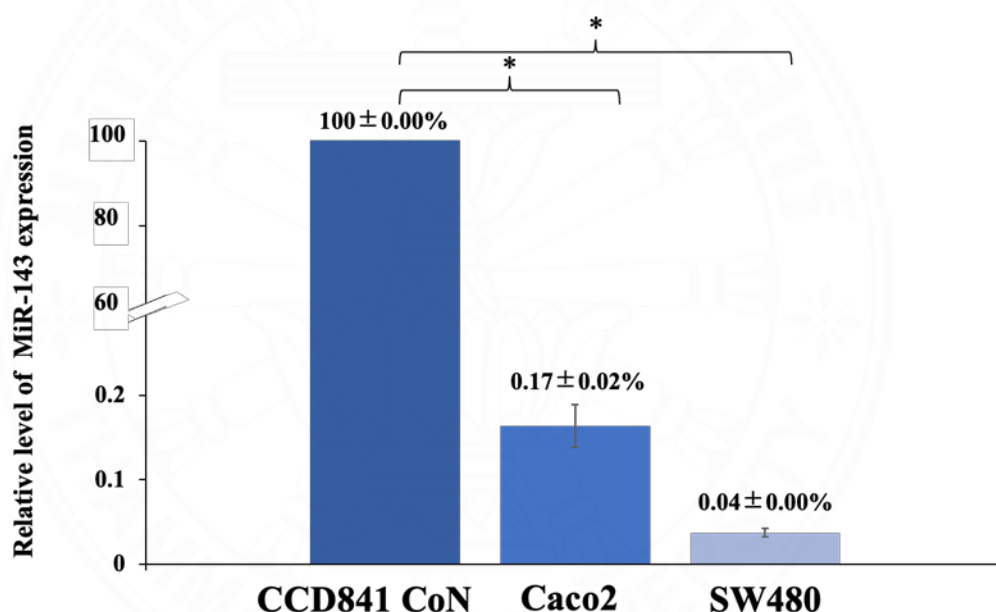


**Figure 4.3** MiR-143 expression was dramatically down-regulated in Caco-2 and SW480 cells, compared to CCD 841 CoN using RT-qPCR analysis.

#### 4.5 *In vitro* cellular uptake of MAH

##### 4.5.1 Study of AS1411 binding capability using a fluorescence microscope

To investigate MAH's binding capabilities, the aptamers were tagged with FAM, a fluorophore, and then treated with MAH and MNH (non-specific aptamers) in SW480 cells. A fluorescent microscope was used to study the treated cells.

Figure 4.4 shows that the cells treated with MAH produced higher fluorescent signals than the cells treated with MNH. This suggested that the AS1411 aptamer could attach to SW480 through an interaction between the aptamer and nucleolin receptors on the cell surface.<sup>129</sup> In contrast, when tested with normal cells (CCD841 CoN), MAH and MNH had no difference in fluorescent intensity under the FAM channel of the microscope (Figure 4.5). As mentioned in the literature, nucleolin proteins are more expressed in cancer cells than in normal cells<sup>130, 131</sup>. Therefore, the results indicated that our hybrid molecule is more specific to cancer cells than to normal cells.

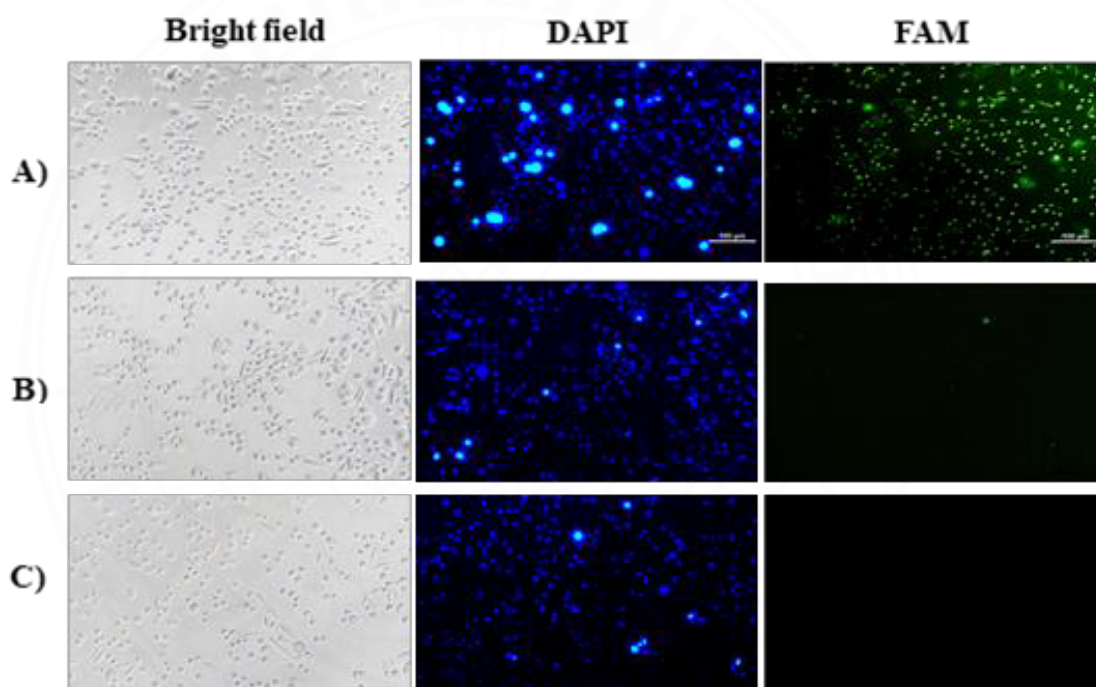


**Figure 4.4** Fluorescent image of (A) SW480 treated with 10  $\mu$ M MAH comprising FAM-labeled AS1411 aptamer, (B) SW480 treated with 10  $\mu$ M MNH comprising FAM-labeled non-specific aptamer, and (C) SW480 without treatment

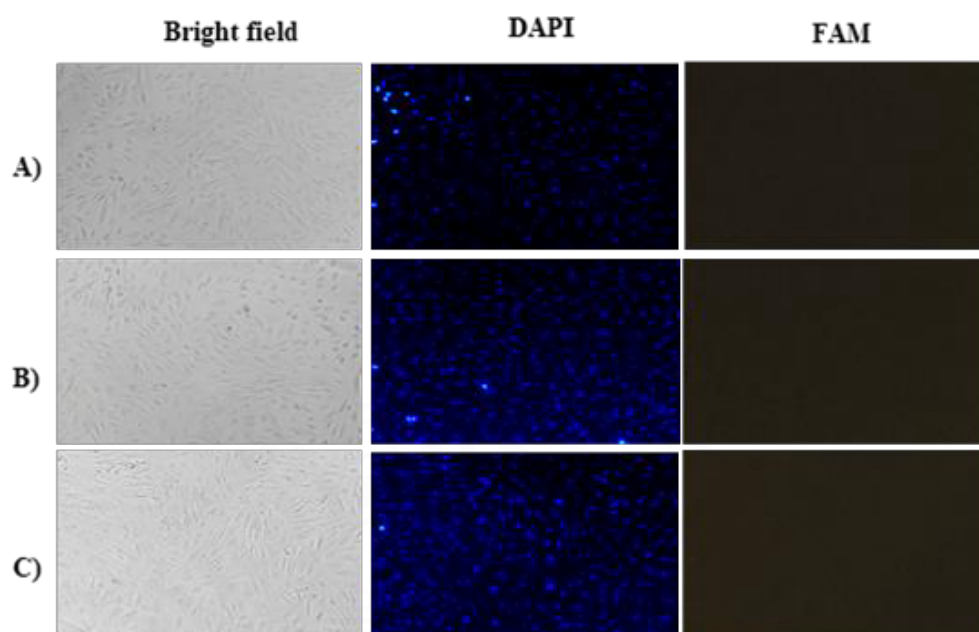


**Figure 4.5** Fluorescent image of (A) CCD 841 CoN treated with 10  $\mu$ M MAH containing FAM-labeled AS1411 aptamer, (B) CCD 841 CoN treated with 10  $\mu$ M MNH containing FAM-labeled non-specific aptamer, and (C) CCD 841 CoN without treatment.

#### 4.5.2 RT-qPCR analysis of exogenous miR-143

To investigate the change of miR-143 levels in SW480 cells, we treated them with MAH and MNH for 48 hours. After testing, it was observed that miR-143 expression levels were significantly higher in MAH-treated cells compared to MNH-treated and untreated cells (Figure 4.6)

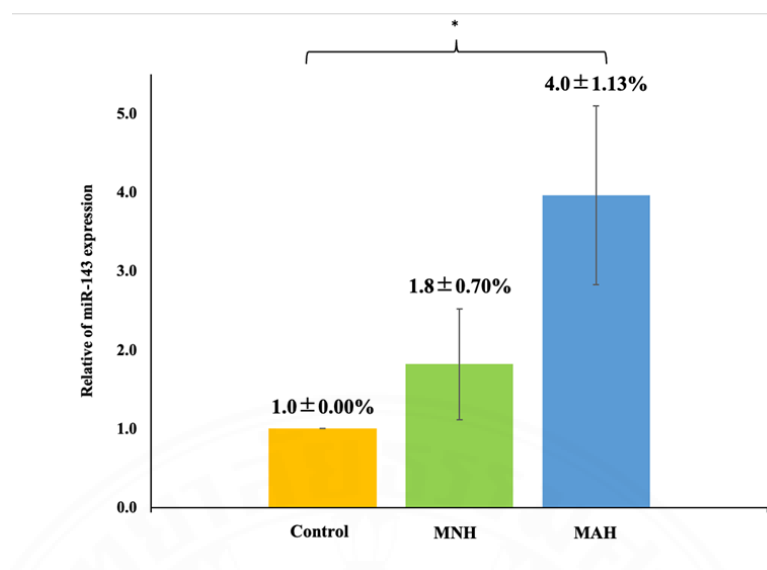


**Figure 4.6** MiR-143 expression rebounded in SW480 cells after treatment with MAH,  $*P < 0.05$ .

## 4.6 Investigation of alteration of miR-143 target gene products

### 4.6.1 *KRAS* mRNA analysis using RT-qPCR in SW480 cells

Previous studies had reported an increase in miR-143 levels after MAH treatment. Thus, we next analyzed *KRAS* gene expression in the SW480 cells. The experimental results revealed that when treated with MAH, the expression of *KRAS* mRNA was significantly lowered, compared to the control (Figure 4.7). MiR-143's target, *KRAS*, has been identified using methods other than computational predictions utilizing tools like TargetScan, miRanda, and PicTar but also through experimental validation<sup>26, 132</sup>.

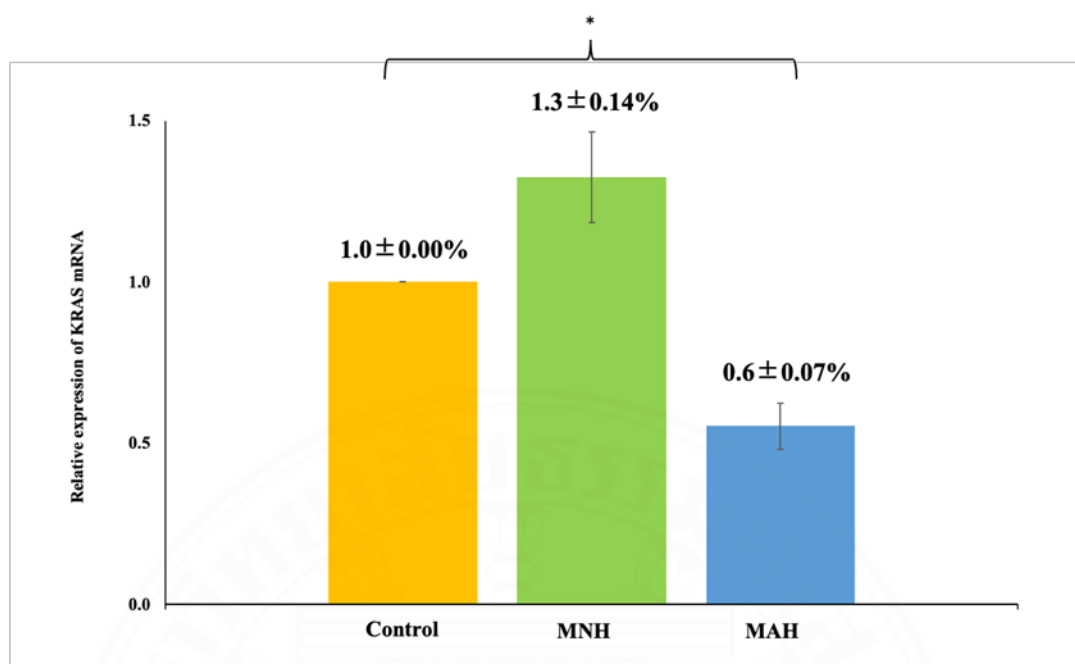
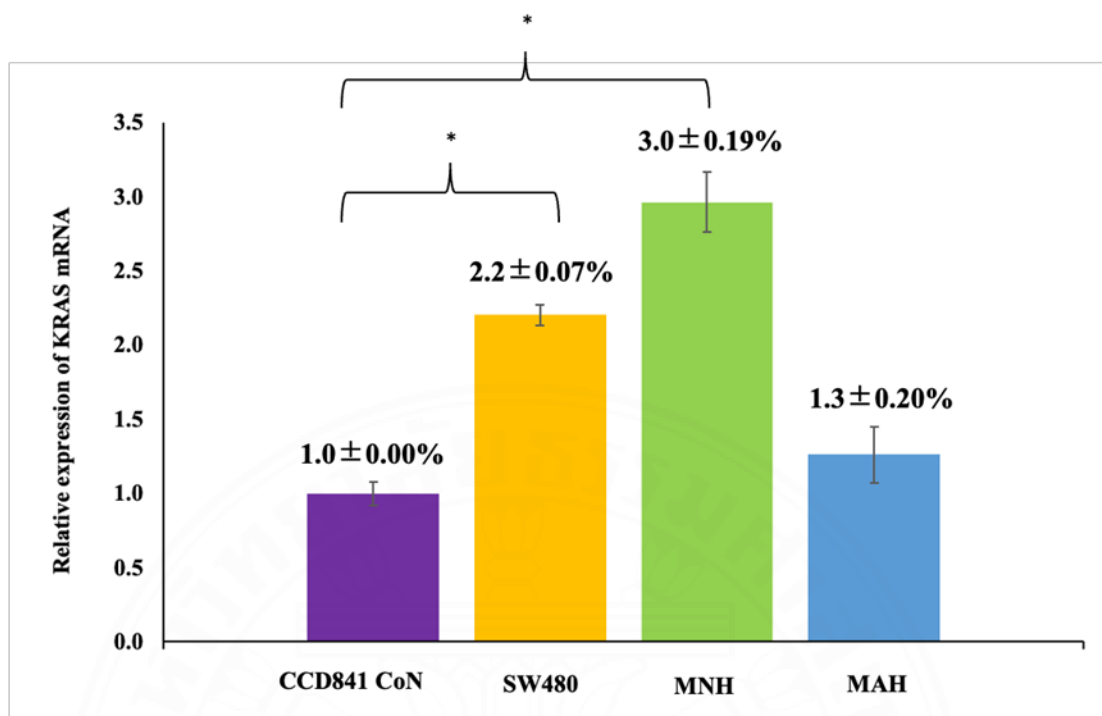


**Figure 4.7** *KRAS* mRNA expression was diminished in SW480 cells after treatment with MAH, \* $P < 0.05$ .

#### 4.6.2 *KRAS* mRNA analysis using RT-qPCR in CCD 841 CoN cells

In this study, we determined *KRAS* mRNA expression in CCD 841 CoN cells by qRT-PCR assay, and then compared it with the MAH-treated SW480 cells. The *KRAS* mRNA expression was reduced dramatically in SW480 cells treated with MAH, similar to the level detected in CCD 841 CoN cells (Figure 4.8). This is consistent with Chen et al. research that reported that overexpression of miR-143 inhibited *KRAS* expression, causing inhibition of constitutive phosphorylation of ERK1/2<sup>26</sup>. Following an examination of *KRAS* expression at the mRNA level, further research was conducted at the protein level.

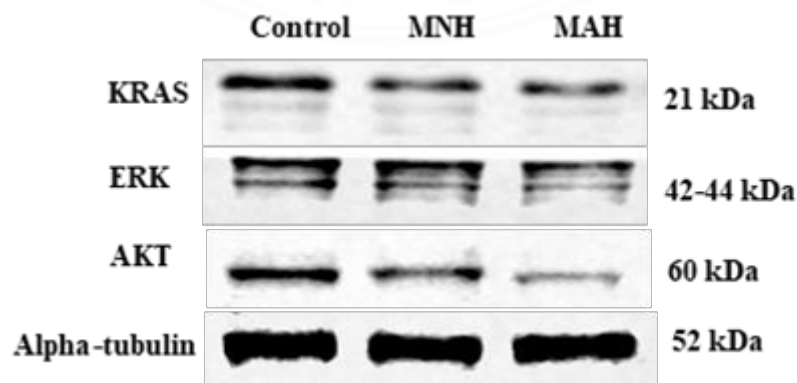




**Figure 4.8** The *KRAS* mRNA level in MAH-treated SW480 cells was comparable to one in CCD 841 CoN, \* $P < 0.05$ .

#### 4.6.3 Western blot analysis of KRAS, AKT and ERK proteins in SW480 cells

Similar to mRNA expression results, it was discovered that SW480 cells treated with MAH had considerably lower KRAS protein levels than untreated cells. In addition, the expression of AKT and ERK, downstream target proteins of  $KRAS^{133, 134}$ , was found to be considerably reduced (Figure 4.9)



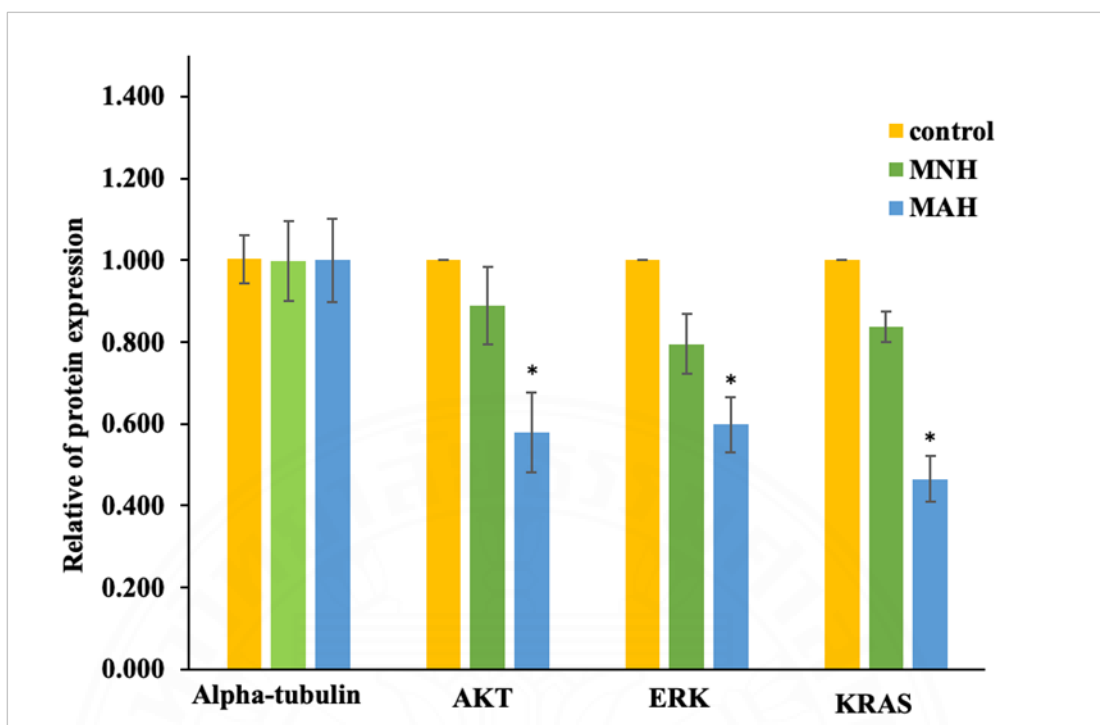


**Figure 4.9** Western blot analysis on SW480 cells for KRAS, AKT, and ERK was treated with MAH, MNH and untreated treatment, respectively, for 72 h, and cell lysate and was detected with antibodies against KRAS, AKT, and ERK. Band intensities were quantitatively analyzed and normalized to  $\alpha$ -tubulin. Data are mean  $\pm$  SD from three replicates using one-way ANOVA (Dunnett's T3 test),  $*P \leq 0.05$  indicates a significant difference

#### 4.7 Intercalation of Dox into MAH

Doxorubicin (Dox) was incorporated into MAH because of its intercalating ability in DNA duplex. The intercalation was evaluated using fluorescence spectroscopy, which monitored the fluorescence quenching of Dox caused by its intercalation in MAH. Fluorescence spectra (Figure 4.10) revealed that Dox exhibited a maximal fluorescence signal at around 590 nm, which was consistent with the results reported in the literature<sup>135</sup>. Furthermore, when mixed with MAH, its fluorescence was entirely suppressed, demonstrating that Dox was successfully inserted. The intercalation is governed by interactions between aromatic moiety in Dox and GC base pairing in our molecular hybrid<sup>136</sup>.

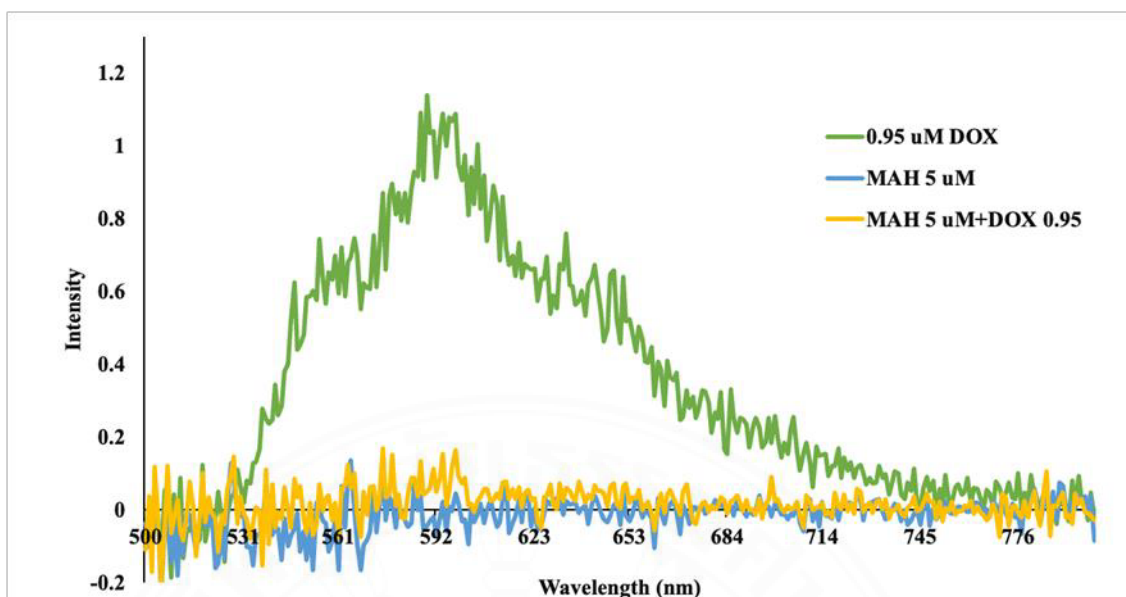


**Figure 4.10** Spectral analysis of free Dox solution fluorescence (0.95  $\mu\text{M}$ ) (green line), MAH (5  $\mu\text{M}$ ) (blue line), and Dox-MAH after incubation for 1.5 hours (yellow line).

#### 4.8 *In vitro* anti-proliferation studies

##### 4.8.1 Effect of Dox-MAH on SW480

To study the effect of Dox-MAH on the proliferation of CRC, SW480 cells were treated with MAH, MNH, Dox-MAH, Dox-MNH, and Dox at IC<sub>50</sub> of Dox on SW480 cells (0.95  $\mu\text{M}$ )<sup>29</sup>, and untreated cells served as a control. Cell viability was determined at 48 hours using the MTS assay. The results showed that Dox-MAH inhibited the proliferation of SW480 cells, which was not significantly different from Dox alone (Figure 4.11). They had similar abilities for suppressing cell growth. Furthermore, SW480 treated with Dox-MAH demonstrated lower cell viability than cells treated with MAH alone, demonstrating Dox toxicity. The cell viability of Dox-MNH-treated cells demonstrated that Dox caused less harm to SW480 when the AS1411 aptamer was not utilized. The results of this study demonstrated that AS1411 aptamer, a recognition and specificity component and facilitator of cellular uptake, can be used to tune the toxicity of Dox to the cells.

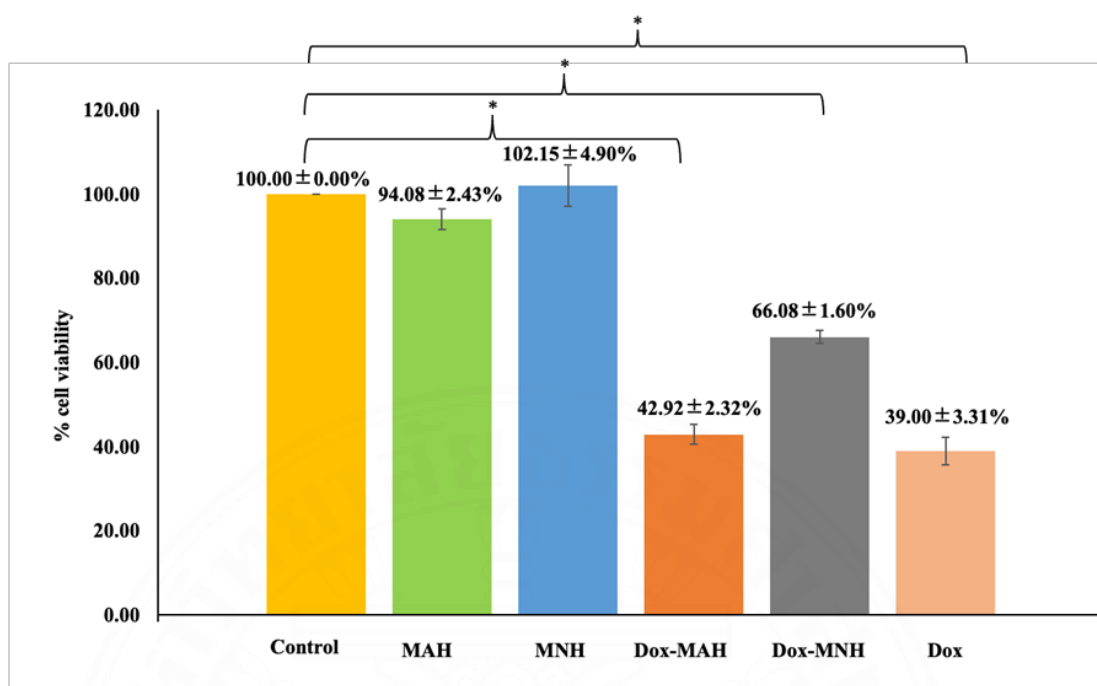


**Figure 4.11** Effect of Dox-MAH on SW480 cell proliferation. The data are shown as mean  $\pm$ SD,  $n=3$ ,  $*P<0.05$ .

#### 4.8.2 Effect of Dox-MAH on CCD 841 CoN

To assess Dox-MAH's impact on normal colon cells, CCD 841 CoN cells were treated with MAH, MNH, Dox-MAH, Dox-MNH, and Dox at the IC<sub>50</sub> of Dox on SW480 cells (0.95  $\mu$ M)<sup>29</sup>, untreated cells served as a reference. The cell viability of each tested sample is shown in Figure 4.12. The results showed that the various treatment molecules were not hazardous to normal colon cells because nucleolin expression on the cell surface is low in normal colon cells<sup>130</sup>. So, AS1411 aptamers were unable to attach and carry substances into the cells. Therefore, Dox-MAH is more toxic to colorectal cancer cells than to normal colon cells.

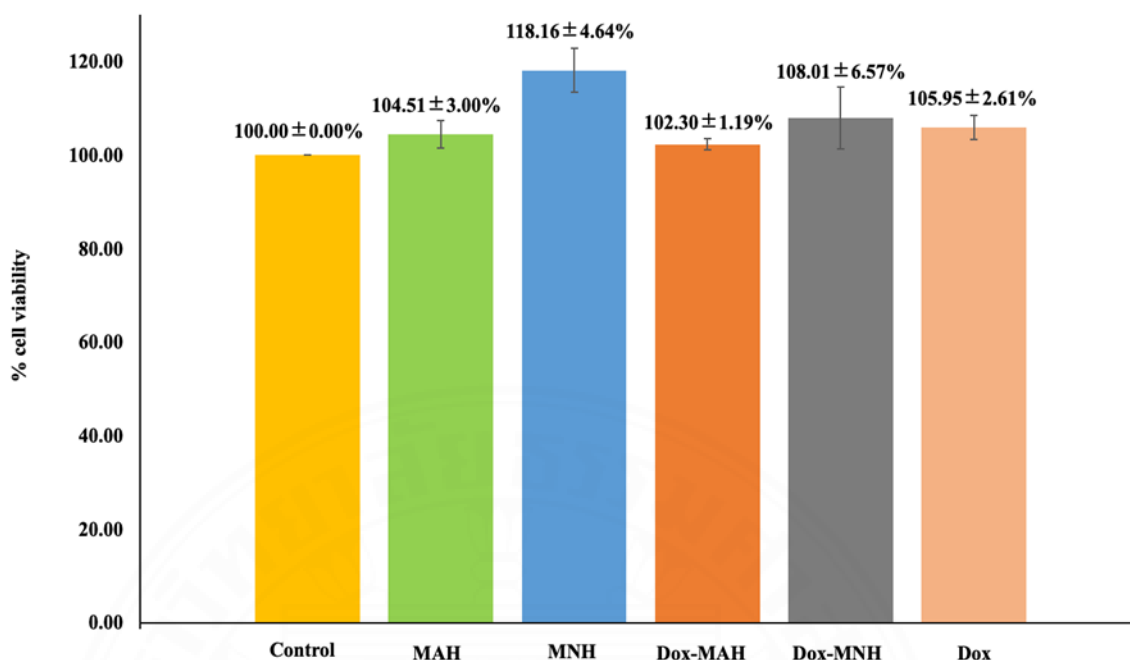


**Figure 4.12** Effect of Dox-MAH on CCD 841 CoN cell proliferation. The data are shown as mean ±SD, n=3, \* $P < 0.05$

#### 4.9 Detection of CRC cell apoptosis after Dox-MAH treatment

To further investigate whether Dox-MAH induces apoptosis, SW480 cells were treated for 48 hours with Dox-MAH, Dox-MNH, and Dox. A flow cytometer was used to evaluate the collected cells, which were double stained with Annexin V-FITC/PI. Flow cytometric data showed that the percentages of viable cells in SW480 cells decreased significantly. Dox-MAH induced cell death through apoptosis, not significantly different from that of Dox. This is demonstrated by a distinct shift from live cells to early and late apoptotic cell populations (Figure 4.13). In contrast, cells treated with Dox-MNH induced significantly fewer apoptosis than cells treated with Dox-MAH and Dox. This confirmed that Dox-MAH could trigger SW480 cell apoptosis and AS1411 aptamer facilitates the uptake of Dox into the SW480 cells.

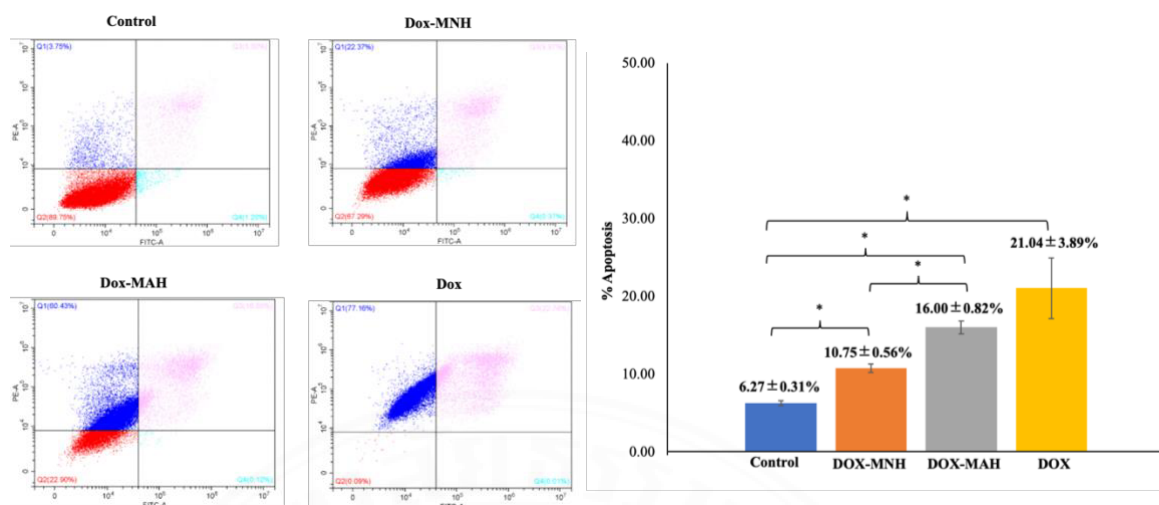


**Figure 4.13** Induction of apoptosis by Dox-MAH on SW480 cells analyzed with a flow cytometer.

#### 4.10 Western blot analysis of proteins in the relevant signaling pathways.

To investigate the mitochondrial-dependent cell death pathway. Western blot analysis was used to examine changes in the protein levels of Bax, Bcl-2, and procaspase-3 in SW480 cells. After SW480 cells were treated for 72 hours as mentioned above, western blot analysis showed that Dox and Dox-MAH induced up-regulation of Bax but significantly down-regulation of Bcl-2 and procaspase-3. Several studies demonstrated that Dox-induced apoptosis in tumor cells. Chemotherapeutic drug-induced death signals result in an inherent apoptotic mechanism driven mostly by the mitochondria. Mitochondrial cytochrome c released into the cytoplasm causes the creation of an apoptosome, a multiprotein complex. Apoptosomes include cytochrome-c, procaspase-9, and the adaptor protein Apaf-1, which cleaves and activates the effector caspase-3, causing cellular death substrates to be degraded<sup>137, 138</sup>. Procaspase-3 expression is lowered when caspase-3 is activated because it is converted to caspase-3. The Bcl-2 family of proteins regulates mitochondrial membrane permeability and can be either pro- or anti-apoptotic. Bcl-2 is an example of an anti-apoptotic protein. Bax is one of the pro-apoptotic proteins.<sup>139</sup>

The experiment findings showed that Dox-MAH and Dox-induced apoptosis due to reduced intensity of anti-apoptotic proteins, Bcl-2 and procaspase-3,

but enhanced Bax intensity, which is a pro-apoptotic protein (Figure 4.14). In contrast, Dox-MNH showed significantly fewer apoptotic signals, suggesting the selectivity of AS1411 aptamer on CRC cells in terms of both targeting and decreasing chemotherapy side effects.

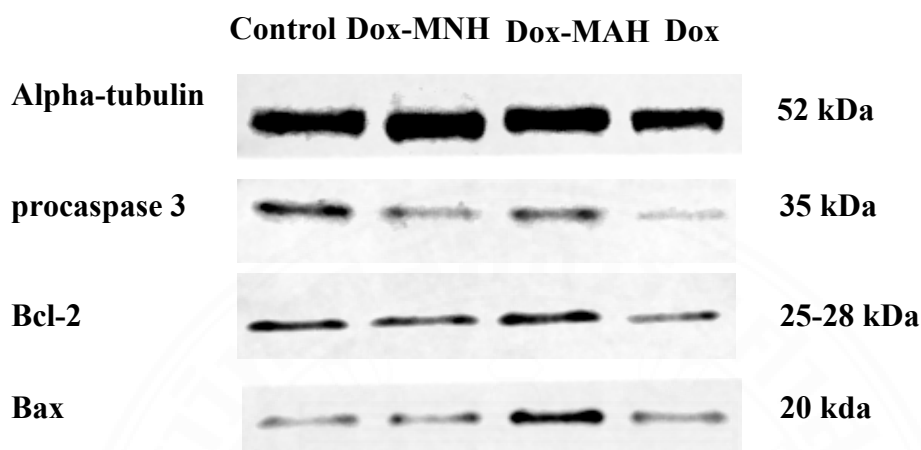


**Figure 4.14** Apoptosis-related protein alterations in SW480 cells after treatment with Dox-MAH, Dox-MNH, Dox and untreated treatment, respectively, for 72 h and cell lysate were detected with antibodies against Bcl-2, Bax, and procaspase-3. Band intensities were quantitatively analyzed and normalized to  $\alpha$ -tubulin. Data are mean  $\pm$  SD from three replicates using one-way ANOVA (Dunnett's T3 test),  $*P \leq 0.05$  indicates a significant difference.

## CHAPTER 5

### CONCLUSIONS AND RECOMMENDATIONS

This master thesis is successful in preparing a smart drug delivery system (SDDSs) of a molecular hybrid (MAH) composed of tumor-suppressor miR-143 and AS1411 aptamer as an anticancer drug carrier. The MAH was produced by combining miR-143 and AS1411 aptamers through a hybridization strand and then loading the molecule with Dox, a chemotherapy drug, in a DNA-RNA duplex. AS1411 aptamer can specifically bind to the nucleolin receptors on SW480 cells, leading to the endocytosis of MAH. The bioavailability and specificity of MAH in SW480 cells were revealed and confirmed by a fluorescence microscope. Upon the treatment of MAH into SW480 cells, the miR-143 level was significantly increased, while oncogenic KRAS mRNA and protein levels were subsequently decreased. In addition, the protein levels of AKT and ERK, the downstream target genes of KRAS and direct target genes of miR-143, were correspondingly diminished. The PI3K/PTEN/AKT and RAF/MEK/ERK pathways play a crucial role in tumorigenesis and chemotherapy drug resistance<sup>38</sup>. Inhibition of these two pathways might benefit CRC chemotherapy. Moreover, Dox-MAH was able to inhibit the proliferation and induce apoptosis in SW480 cells. Dox-MAH increased apoptosis by disrupting the permeability of the mitochondrial outer membrane and activating caspase-3 as a result, as evidenced by a rise in pro-apoptotic Bax and a decrease in anti-apoptotic Bcl-2 and procaspase-3 proteins.

However, the limitation of this research is the reduction of adverse effects such as cardiotoxicity was not directly proved. We know only that AS1411 facilitated the specificity of MAH to the CRC cells, and Dox was not harmful to normal colon cells. Consequently, further investigation on the direct effects of Dox-MAH on target tissues such as cardiac muscle and endothelial cells should be done in animal models (*in vivo*). Such a finding would be helpful to confirm not only the capability of Dox-MAH molecule in lessening the adverse effects but also the effectiveness in cancer treatments.



In summary, this study demonstrated a new targeted drug delivery system using MAH as Dox and miR-143 carrier. Hopefully, therapeutic efficacy could be increased due to SDDSs' ability.



## REFERENCES

- (1) Sung, H.; Ferlay, J.; Siegel, R. L.; Laversanne, M.; Soerjomataram, I.; Jemal, A.; Bray, F. Global Cancer Statistics 2020: GLOBOCAN Estimates of Incidence and Mortality Worldwide for 36 Cancers in 185 Countries. *CA: A Cancer Journal for Clinicians* **2021**, *71* (3), 209-249, <https://doi.org/10.3322/caac.21660>. DOI: <https://doi.org/10.3322/caac.21660> (accessed 2023/07/17).
- (2) Siegel, R. L.; Wagle, N. S.; Cercek, A.; Smith, R. A.; Jemal, A. Colorectal cancer statistics, 2023. *CA: A Cancer Journal for Clinicians* **2023**, *73* (3), 233-254. DOI: <https://doi.org/10.3322/caac.21772>.
- (3) Siegel, R. L.; Miller, K. D.; Goding Sauer, A.; Fedewa, S. A.; Butterly, L. F.; Anderson, J. C.; Cercek, A.; Smith, R. A.; Jemal, A. Colorectal cancer statistics, 2020. *CA Cancer J Clin* **2020**, *70* (3), 145-164. DOI: 10.3322/caac.21601 From NLM.
- (4) Xia, C.; Dong, X.; Li, H.; Cao, M.; Sun, D.; He, S.; Yang, F.; Yan, X.; Zhang, S.; Li, N.; et al. Cancer statistics in China and United States, 2022: profiles, trends, and determinants. *Chin Med J (Engl)* **2022**, *135* (5), 584-590. DOI: 10.1097/cm9.0000000000002108 From NLM.
- (5) Unit, M. R. a. D. C. *hospital-based cancer registry 2021*; แสงอรุณวิช., น. ., Ed.; Medical Digital Division National Cancer Institute, 2022.
- (6) Shukla, S.; Allam, U. S.; Ahsan, A.; Chen, G.; Krishnamurthy, P. M.; Marsh, K.; Rumschlag, M.; Shankar, S.; Whitehead, C.; Schipper, M.; et al. KRAS protein stability is regulated through SMURF2: UBC5 complex-mediated  $\beta$ -TrCP1 degradation. *Neoplasia* **2014**, *16* (2), 115-128. DOI: 10.1593/neo.14184 From NLM.
- (7) Van Cutsem, E.; Lenz, H. J.; Köhne, C. H.; Heinemann, V.; Tejpar, S.; Melezínek, I.; Beier, F.; Stroh, C.; Rougier, P.; van Krieken, J. H.; et al. Fluorouracil, leucovorin, and irinotecan plus cetuximab treatment and RAS mutations in colorectal cancer. *J Clin Oncol* **2015**, *33* (7), 692-700. DOI: 10.1200/jco.2014.59.4812 From NLM.
- (8) Liu, H.; Liu, J.; Huo, J.; Li, K.; Li, K.; Guo, H.; Yang, Y. Downregulation of miR-143 modulates KRAS expression in colorectal carcinoma cells. *Oncol Rep* **2019**, *42* (6), 2759-2767. DOI: 10.3892/or.2019.7359 From NLM.

- (9) Piawah, S.; Venook, A. P. Targeted therapy for colorectal cancer metastases: A review of current methods of molecularly targeted therapy and the use of tumor biomarkers in the treatment of metastatic colorectal cancer. *Cancer* **2019**, *125* (23), 4139-4147. DOI: 10.1002/cncr.32163 From NLM.
- (10) Ganesh, K.; Stadler, Z. K.; Cercek, A.; Mendelsohn, R. B.; Shia, J.; Segal, N. H.; Diaz, L. A., Jr. Immunotherapy in colorectal cancer: rationale, challenges and potential. *Nat Rev Gastroenterol Hepatol* **2019**, *16* (6), 361-375. DOI: 10.1038/s41575-019-0126-x From NLM.
- (11) Haraldsdottir, S.; Einarsdottir, H. M.; Smaradottir, A.; Gunnlaugsson, A.; Halfdanarson, T. R. [Colorectal cancer - review]. *Laeknabladid* **2014**, *100* (2), 75-82. DOI: 10.17992/lbl.2014.02.531 From NLM.
- (12) Zhao, N.; Woodle, M. C.; Mixson, A. J. Advances in delivery systems for doxorubicin. *J Nanomed Nanotechnol* **2018**, *9* (5). DOI: 10.4172/2157-7439.1000519 From NLM.
- (13) Thorn, C. F.; Oshiro, C.; Marsh, S.; Hernandez-Boussard, T.; McLeod, H.; Klein, T. E.; Altman, R. B. Doxorubicin pathways: pharmacodynamics and adverse effects. *Pharmacogenet Genomics* **2011**, *21* (7), 440-446. DOI: 10.1097/FPC.0b013e32833ffb56 From NLM.
- (14) Chabner, B. A.; Roberts, T. G., Jr. Timeline: Chemotherapy and the war on cancer. *Nat Rev Cancer* **2005**, *5* (1), 65-72. DOI: 10.1038/nrc1529 From NLM.
- (15) Hanahan, D.; Weinberg, R. A. Hallmarks of cancer: the next generation. *Cell* **2011**, *144* (5), 646-674. DOI: 10.1016/j.cell.2011.02.013 From NLM.
- (16) Pérez-Herrero, E.; Fernández-Medarde, A. Advanced targeted therapies in cancer: Drug nanocarriers, the future of chemotherapy. *Eur J Pharm Biopharm* **2015**, *93*, 52-79. DOI: 10.1016/j.ejpb.2015.03.018 From NLM.
- (17) Breaker, R. R. DNA aptamers and DNA enzymes. *Curr Opin Chem Biol* **1997**, *1* (1), 26-31. DOI: 10.1016/s1367-5931(97)80105-6 From NLM.
- (18) Xu, Y.; Jiang, X.; Zhou, Y.; Ma, M.; Wang, M.; Ying, B. Systematic Evolution of Ligands by Exponential Enrichment Technologies and Aptamer-Based Applications: Recent Progress and Challenges in Precision Medicine of Infectious Diseases. *Front Bioeng Biotechnol* **2021**, *9*, 704077. DOI: 10.3389/fbioe.2021.704077 From NLM.

- (19) Wu, X.; Shaikh, A. B.; Yu, Y.; Li, Y.; Ni, S.; Lu, A.; Zhang, G. Potential Diagnostic and Therapeutic Applications of Oligonucleotide Aptamers in Breast Cancer. *Int J Mol Sci* **2017**, *18* (9). DOI: 10.3390/ijms18091851 From NLM.
- (20) Reyes-Reyes, E. M.; Teng, Y.; Bates, P. J. A new paradigm for aptamer therapeutic AS1411 action: uptake by macropinocytosis and its stimulation by a nucleolin-dependent mechanism. *Cancer Res* **2010**, *70* (21), 8617-8629. DOI: 10.1158/0008-5472.Can-10-0920 From NLM.
- (21) Bartel, D. P. MicroRNAs: target recognition and regulatory functions. *Cell* **2009**, *136* (2), 215-233. DOI: 10.1016/j.cell.2009.01.002 From NLM.
- (22) Vasudevan, S.; Tong, Y.; Steitz, J. A. Switching from repression to activation: microRNAs can up-regulate translation. *Science* **2007**, *318* (5858), 1931-1934. DOI: 10.1126/science.1149460 From NLM.
- (23) Guo, H.; Chen, Y.; Hu, X.; Qian, G.; Ge, S.; Zhang, J. The regulation of Toll-like receptor 2 by miR-143 suppresses the invasion and migration of a subset of human colorectal carcinoma cells. *Mol Cancer* **2013**, *12*, 77. DOI: 10.1186/1476-4598-12-77 From NLM.
- (24) Wang, L.; Shi, Z. M.; Jiang, C. F.; Liu, X.; Chen, Q. D.; Qian, X.; Li, D. M.; Ge, X.; Wang, X. F.; Liu, L. Z.; et al. MiR-143 acts as a tumor suppressor by targeting N-RAS and enhances temozolomide-induced apoptosis in glioma. *Oncotarget* **2014**, *5* (14), 5416-5427. DOI: 10.18632/oncotarget.2116 From NLM.
- (25) Zhang, H.; Cai, X.; Wang, Y.; Tang, H.; Tong, D.; Ji, F. microRNA-143, down-regulated in osteosarcoma, promotes apoptosis and suppresses tumorigenicity by targeting Bcl-2. *Oncol Rep* **2010**, *24* (5), 1363-1369. DOI: 10.3892/or\_00000994 From NLM.
- (26) Chen, X.; Guo, X.; Zhang, H.; Xiang, Y.; Chen, J.; Yin, Y.; Cai, X.; Wang, K.; Wang, G.; Ba, Y.; et al. Role of miR-143 targeting KRAS in colorectal tumorigenesis. *Oncogene* **2009**, *28* (10), 1385-1392. DOI: 10.1038/onc.2008.474 From NLM.
- (27) Zhang, Y.; Wang, Z.; Chen, M.; Peng, L.; Wang, X.; Ma, Q.; Ma, F.; Jiang, B. MicroRNA-143 targets MACC1 to inhibit cell invasion and migration in colorectal cancer. *Mol Cancer* **2012**, *11*, 23. DOI: 10.1186/1476-4598-11-23 From NLM.

- (28) Michael, M. Z.; SM, O. C.; van Holst Pellekaan, N. G.; Young, G. P.; James, R. J. Reduced accumulation of specific microRNAs in colorectal neoplasia. *Mol Cancer Res* **2003**, *1* (12), 882-891. From NLM.
- (29) Rotkrua, P.; Lohlamoh, W.; Watcharapo, P.; Soontornworajit, B. A molecular hybrid comprising AS1411 and PDGF-BB aptamer, cholesterol, and doxorubicin for inhibiting proliferation of SW480 cells. *J Mol Recognit* **2021**, *34* (11), e2926. DOI: 10.1002/jmr.2926 From NLM.
- (30) Siegel, R. L.; Miller, K. D.; Fuchs, H. E.; Jemal, A. Cancer statistics, 2022. *CA Cancer J Clin* **2022**, *72* (1), 7-33. DOI: 10.3322/caac.21708 From NLM.
- (31) team, T. A. C. S. m. a. e. c. *About Colorectal Cancer*. 2020. <https://www.cancer.org/content/dam/CRC/PDF/Public/8604.00.pdf> (accessed 2023).
- (32) team, T. A. C. S. m. a. e. c. *Colorectal Cancer Causes, Risk Factors, and Prevention*. 2020. <https://www.cancer.org/content/dam/CRC/PDF/Public/8605.00.pdf> (accessed 2023).
- (33) Sakai, E.; Nakayama, M.; Oshima, H.; Kouyama, Y.; Niida, A.; Fujii, S.; Ochiai, A.; Nakayama, K. I.; Mimori, K.; Suzuki, Y.; et al. Combined Mutation of Apc, Kras, and Tgfr2 Effectively Drives Metastasis of Intestinal Cancer. *Cancer Res* **2018**, *78* (5), 1334-1346. DOI: 10.1158/0008-5472.Can-17-3303 From NLM.
- (34) Jeong, W. J.; Ro, E. J.; Choi, K. Y. Interaction between Wnt/ $\beta$ -catenin and RAS-ERK pathways and an anti-cancer strategy via degradations of  $\beta$ -catenin and RAS by targeting the Wnt/ $\beta$ -catenin pathway. *NPJ Precis Oncol* **2018**, *2* (1), 5. DOI: 10.1038/s41698-018-0049-y From NLM.
- (35) Wen, J.; Min, X.; Shen, M.; Hua, Q.; Han, Y.; Zhao, L.; Liu, L.; Huang, G.; Liu, J.; Zhao, X. ACLY facilitates colon cancer cell metastasis by CTNNB1. *J Exp Clin Cancer Res* **2019**, *38* (1), 401. DOI: 10.1186/s13046-019-1391-9 From NLM.
- (36) Huang, Y.; Chen, Z.; Lu, T.; Bi, G.; Li, M.; Liang, J.; Hu, Z.; Zheng, Y.; Yin, J.; Xi, J.; et al. HIF-1 $\alpha$  switches the functionality of TGF- $\beta$  signaling via changing the partners of smads to drive glucose metabolic reprogramming in non-small cell lung cancer. *J Exp Clin Cancer Res* **2021**, *40* (1), 398. DOI: 10.1186/s13046-021-02188-y From NLM.
- (37) Díez-Alonso, M.; Mendoza-Moreno, F.; Gómez-Sanz, R.; Matías-García, B.; Ovejero-Merino, E.; Molina, R.; Soto-Schütte, S.; San Juan, A.; Gutierrez-Calvo, A.

Prognostic Value of KRAS Gene Mutation on Survival of Patients with Peritoneal Metastases of Colorectal Adenocarcinoma. *Int J Surg Oncol* **2021**, 2021, 3946875. DOI: 10.1155/2021/3946875 From NLM.

(38) McCubrey, J. A.; Steelman, L. S.; Abrams, S. L.; Lee, J. T.; Chang, F.; Bertrand, F. E.; Navolanic, P. M.; Terrian, D. M.; Franklin, R. A.; D'Assoro, A. B.; et al. Roles of the RAF/MEK/ERK and PI3K/PTEN/AKT pathways in malignant transformation and drug resistance. *Adv Enzyme Regul* **2006**, 46, 249-279. DOI: 10.1016/j.advenzreg.2006.01.004 From NLM.

(39) Sugito, N.; Heishima, K.; Akao, Y. Chemically modified MIR143-3p exhibited anti-cancer effects by impairing the KRAS network in colorectal cancer cells. *Mol Ther Nucleic Acids* **2022**, 30, 49-61. DOI: 10.1016/j.omtn.2022.09.001 From NLM.

(40) Dassie, J. P.; Liu, X. Y.; Thomas, G. S.; Whitaker, R. M.; Thiel, K. W.; Stockdale, K. R.; Meyerholz, D. K.; McCaffrey, A. P.; McNamara, J. O., 2nd; Giangrande, P. H. Systemic administration of optimized aptamer-siRNA chimeras promotes regression of PSMA-expressing tumors. *Nat Biotechnol* **2009**, 27 (9), 839-849. DOI: 10.1038/nbt.1560 From NLM.

(41) Tuerk, C.; Gold, L. Systematic evolution of ligands by exponential enrichment: RNA ligands to bacteriophage T4 DNA polymerase. *Science* **1990**, 249 (4968), 505-510. DOI: 10.1126/science.2200121 From NLM.

(42) Micura, R.; Höbartner, C. Fundamental studies of functional nucleic acids: aptamers, riboswitches, ribozymes and DNazymes. *Chemical Society Reviews* **2020**, 49 (20), 7331-7353, 10.1039/D0CS00617C. DOI: 10.1039/D0CS00617C.

(43) Stoltenburg, R.; Reinemann, C.; Strehlitz, B. SELEX--a (r)evolutionary method to generate high-affinity nucleic acid ligands. *Biomol Eng* **2007**, 24 (4), 381-403. DOI: 10.1016/j.bioeng.2007.06.001 From NLM.

(44) Vant-Hull, B.; Gold, L.; Zichi, D. A. Theoretical principles of in vitro selection using combinatorial nucleic acid libraries. *Curr Protoc Nucleic Acid Chem* **2000**, Chapter 9, Unit 9.1. DOI: 10.1002/0471142700.nc0901s00 From NLM.

(45) Hall, B.; Arshad, S.; Seo, K.; Bowman, C.; Corley, M.; Jhaveri, S. D.; Ellington, A. D. In vitro selection of RNA aptamers to a protein target by filter immobilization. *Curr Protoc Mol Biol* **2009**, Chapter 24, Unit 24.23. DOI: 10.1002/0471142727.mb2403s88 From NLM.

- (46) Gopinath, S. C. Methods developed for SELEX. *Anal Bioanal Chem* **2007**, 387 (1), 171-182. DOI: 10.1007/s00216-006-0826-2 From NLM.
- (47) Shi, H.; Kou, Q.; Wu, P.; Sun, Q.; Wu, J.; Le, T. Selection and Application of DNA Aptamers Against Sulfaquinoxaline Assisted by Graphene Oxide–Based SELEX. *Food Analytical Methods* **2021**, 14, 1-10. DOI: 10.1007/s12161-020-01869-2.
- (48) Kaur, H. Recent developments in cell-SELEX technology for aptamer selection. *Biochim Biophys Acta Gen Subj* **2018**, 1862 (10), 2323-2329. DOI: 10.1016/j.bbagen.2018.07.029 From NLM.
- (49) Mayer, G.; Ahmed, M. S.; Dolf, A.; Endl, E.; Knolle, P. A.; Famulok, M. Fluorescence-activated cell sorting for aptamer SELEX with cell mixtures. *Nat Protoc* **2010**, 5 (12), 1993-2004. DOI: 10.1038/nprot.2010.163 From NLM.
- (50) Khan, H.; Missailidis, S. Aptamers in oncology: A diagnostic perspective. *Gene Therapy and Molecular Biology* **2008**, 12.
- (51) Stoltenburg, R.; Nikolaus, N.; Strehlitz, B. Capture-SELEX: Selection of DNA Aptamers for Aminoglycoside Antibiotics. *Journal of Analytical Methods in Chemistry* **2012**, 2012, 415697. DOI: 10.1155/2012/415697.
- (52) Chen, T.; Shukoor, M. I.; Chen, Y.; Yuan, Q.; Zhu, Z.; Zhao, Z.; Gulbakan, B.; Tan, W. Aptamer-conjugated nanomaterials for bioanalysis and biotechnology applications. *Nanoscale* **2011**, 3 (2), 546-556, 10.1039/C0NR00646G. DOI: 10.1039/C0NR00646G.
- (53) Ireson, C. R.; Kelland, L. R. Discovery and development of anticancer aptamers. *Mol Cancer Ther* **2006**, 5 (12), 2957-2962. DOI: 10.1158/1535-7163.Mct-06-0172 From NLM.
- (54) Keefe, A. D.; Pai, S.; Ellington, A. Aptamers as therapeutics. *Nature Reviews Drug Discovery* **2010**, 9 (7), 537-550. DOI: 10.1038/nrd3141.
- (55) Sun, H.; Zu, Y. Aptamers and their applications in nanomedicine. *Small* **2015**, 11 (20), 2352-2364. DOI: 10.1002/smll.201403073 From NLM.
- (56) Gragoudas, E. S.; Adamis, A. P.; Cunningham, E. T., Jr.; Feinsod, M.; Guyer, D. R. Pegaptanib for neovascular age-related macular degeneration. *N Engl J Med* **2004**, 351 (27), 2805-2816. DOI: 10.1056/NEJMoa042760 From NLM.



- (57) Kolb, G.; Reigadas, S.; Castanotto, D.; Faure, A.; Ventura, M.; Rossi, J. J.; Toulmé, J. J. Endogenous expression of an anti-TAR aptamer reduces HIV-1 replication. *RNA Biol* **2006**, *3* (4), 150-156. DOI: 10.4161/rna.3.4.3811 From NLM.
- (58) Yang, S.; Li, H.; Xu, L.; Deng, Z.; Han, W.; Liu, Y.; Jiang, W.; Zu, Y. Oligonucleotide Aptamer-Mediated Precision Therapy of Hematological Malignancies. *Mol Ther Nucleic Acids* **2018**, *13*, 164-175. DOI: 10.1016/j.omtn.2018.08.023 From NLM.
- (59) Dou, B.; Xu, L.; Jiang, B.; Yuan, R.; Xiang, Y. Aptamer-Functionalized and Gold Nanoparticle Array-Decorated Magnetic Graphene Nanosheets Enable Multiplexed and Sensitive Electrochemical Detection of Rare Circulating Tumor Cells in Whole Blood. *Anal Chem* **2019**, *91* (16), 10792-10799. DOI: 10.1021/acs.analchem.9b02403 From NLM.
- (60) Toscano-Garibay, J. D.; Benítez-Hess, M. L.; Alvarez-Salas, L. M. Isolation and characterization of an RNA aptamer for the HPV-16 E7 oncoprotein. *Arch Med Res* **2011**, *42* (2), 88-96. DOI: 10.1016/j.arcmed.2011.02.005 From NLM.
- (61) Li, X.; An, Y.; Jin, J.; Zhu, Z.; Hao, L.; Liu, L.; Shi, Y.; Fan, D.; Ji, T.; Yang, C. J. Evolution of DNA aptamers through in vitro metastatic-cell-based systematic evolution of ligands by exponential enrichment for metastatic cancer recognition and imaging. *Anal Chem* **2015**, *87* (9), 4941-4948. DOI: 10.1021/acs.analchem.5b00637 From NLM.
- (62) Subramanian, N.; Raghunathan, V.; Kanwar, J. R.; Kanwar, R. K.; Elchuri, S. V.; Khetan, V.; Krishnakumar, S. Target-specific delivery of doxorubicin to retinoblastoma using epithelial cell adhesion molecule aptamer. *Mol Vis* **2012**, *18*, 2783-2795. From NLM.
- (63) Han, J.; Gao, L.; Wang, J.; Wang, J. Application and development of aptamer in cancer: from clinical diagnosis to cancer therapy. *J Cancer* **2020**, *11* (23), 6902-6915. DOI: 10.7150/jca.49532 From NLM.
- (64) Zhu, G.; Chen, X. Aptamer-based targeted therapy. *Adv Drug Deliv Rev* **2018**, *134*, 65-78. DOI: 10.1016/j.addr.2018.08.005 From NLM.
- (65) Agudelo, D.; Bourassa, P.; Bérubé, G.; Tajmir-Riahi, H. A. Review on the binding of anticancer drug doxorubicin with DNA and tRNA: Structural models and antitumor



activity. *Journal of Photochemistry and Photobiology B: Biology* **2016**, *158*, 274-279. DOI: <https://doi.org/10.1016/j.jphotobiol.2016.02.032>.

(66) Huang, Y. F.; Shangguan, D.; Liu, H.; Phillips, J. A.; Zhang, X.; Chen, Y.; Tan, W. Molecular assembly of an aptamer-drug conjugate for targeted drug delivery to tumor cells. *Chembiochem* **2009**, *10* (5), 862-868. DOI: 10.1002/cbic.200800805 From NLM.

(67) Dai, F.; Zhang, Y.; Zhu, X.; Shan, N.; Chen, Y. Anticancer role of MUC1 aptamer-miR-29b chimera in epithelial ovarian carcinoma cells through regulation of PTEN methylation. *Target Oncol* **2012**, *7* (4), 217-225. DOI: 10.1007/s11523-012-0236-7 From NLM.

(68) Russo, V.; Paciocco, A.; Affinito, A.; Roscigno, G.; Fiore, D.; Palma, F.; Galasso, M.; Volinia, S.; Fiorelli, A.; Esposito, C. L.; et al. Aptamer-miR-34c Conjugate Affects Cell Proliferation of Non-Small-Cell Lung Cancer Cells. *Molecular Therapy - Nucleic Acids* **2018**, *13*, 334-346. DOI: <https://doi.org/10.1016/j.omtn.2018.09.016>.

(69) Bates, P. J.; Laber, D. A.; Miller, D. M.; Thomas, S. D.; Trent, J. O. Discovery and development of the G-rich oligonucleotide AS1411 as a novel treatment for cancer. *Exp Mol Pathol* **2009**, *86* (3), 151-164. DOI: 10.1016/j.yexmp.2009.01.004 From NLM.

(70) Teng, Y.; Girvan, A. C.; Casson, L. K.; Pierce, W. M., Jr.; Qian, M.; Thomas, S. D.; Bates, P. J. AS1411 alters the localization of a complex containing protein arginine methyltransferase 5 and nucleolin. *Cancer Res* **2007**, *67* (21), 10491-10500. DOI: 10.1158/0008-5472.Can-06-4206 From NLM.

(71) Soundararajan, S.; Chen, W.; Spicer, E. K.; Courtenay-Luck, N.; Fernandes, D. J. The nucleolin targeting aptamer AS1411 destabilizes Bcl-2 messenger RNA in human breast cancer cells. *Cancer Res* **2008**, *68* (7), 2358-2365. DOI: 10.1158/0008-5472.Can-07-5723 From NLM.

(72) Mongelard, F.; Bouvet, P. AS-1411, a guanosine-rich oligonucleotide aptamer targeting nucleolin for the potential treatment of cancer, including acute myeloid leukemia. *Curr Opin Mol Ther* **2010**, *12* (1), 107-114. From NLM.

(73) Reyes-Reyes, E. M.; Šalipur, F. R.; Shams, M.; Forsthoefel, M. K.; Bates, P. J. Mechanistic studies of anticancer aptamer AS1411 reveal a novel role for nucleolin in regulating Rac1 activation. *Mol Oncol* **2015**, *9* (7), 1392-1405. DOI: 10.1016/j.molonc.2015.03.012 From NLM.

- (74) Abdelmohsen, K.; Gorospe, M. RNA-binding protein nucleolin in disease. *RNA Biol* **2012**, *9* (6), 799-808. DOI: 10.4161/rna.19718 From NLM.
- (75) Tong, X.; Ga, L.; Ai, J.; Wang, Y. Progress in cancer drug delivery based on AS1411 oriented nanomaterials. *J Nanobiotechnology* **2022**, *20* (1), 57. DOI: 10.1186/s12951-022-01240-z From NLM.
- (76) Carvalho, J.; Paiva, A.; Cabral Campello, M. P.; Paulo, A.; Mergny, J. L.; Salgado, G. F.; Queiroz, J. A.; Cruz, C. Aptamer-based Targeted Delivery of a G-quadruplex Ligand in Cervical Cancer Cells. *Sci Rep* **2019**, *9* (1), 7945. DOI: 10.1038/s41598-019-44388-9 From NLM.
- (77) Davidson, B. L.; McCray, P. B., Jr. Current prospects for RNA interference-based therapies. *Nat Rev Genet* **2011**, *12* (5), 329-340. DOI: 10.1038/nrg2968 From NLM.
- (78) Esposito, C. L.; Nuzzo, S.; Kumar, S. A.; Rienzo, A.; Lawrence, C. L.; Pallini, R.; Shaw, L.; Alder, J. E.; Ricci-Vitiani, L.; Catuogno, S.; et al. A combined microRNA-based targeted therapeutic approach to eradicate glioblastoma stem-like cells. *Journal of Controlled Release* **2016**, *238*, 43-57. DOI: <https://doi.org/10.1016/j.jconrel.2016.07.032>.
- (79) Vandghanooni, S.; Eskandani, M.; Barar, J.; Omid, Y. AS1411 aptamer-decorated cisplatin-loaded poly(lactic-co-glycolic acid) nanoparticles for targeted therapy of miR-21-inhibited ovarian cancer cells. *Nanomedicine (Lond)* **2018**, *13* (21), 2729-2758. DOI: 10.2217/nnm-2018-0205 From NLM.
- (80) Zhou, J.; Rossi, J. J. Cell-type-specific, Aptamer-functionalized Agents for Targeted Disease Therapy. *Mol Ther Nucleic Acids* **2014**, *3* (6), e169. DOI: 10.1038/mtna.2014.21 From NLM.
- (81) Trinh, T. L.; Zhu, G.; Xiao, X.; Puszyk, W.; Sefah, K.; Wu, Q.; Tan, W.; Liu, C. A Synthetic Aptamer-Drug Adduct for Targeted Liver Cancer Therapy. *PLoS One* **2015**, *10* (11), e0136673. DOI: 10.1371/journal.pone.0136673 From NLM.
- (82) Lewis, B. P.; Burge, C. B.; Bartel, D. P. Conserved seed pairing, often flanked by adenosines, indicates that thousands of human genes are microRNA targets. *Cell* **2005**, *120* (1), 15-20. DOI: 10.1016/j.cell.2004.12.035 From NLM.
- (83) Filipowicz, W. RNAi: the nuts and bolts of the RISC machine. *Cell* **2005**, *122* (1), 17-20. DOI: 10.1016/j.cell.2005.06.023 From NLM.

- (84) Lee, R. C.; Feinbaum, R. L.; Ambros, V. The *C. elegans* heterochronic gene *lin-4* encodes small RNAs with antisense complementarity to *lin-14*. *Cell* **1993**, *75* (5), 843-854. DOI: 10.1016/0092-8674(93)90529-y From NLM.
- (85) Wightman, B.; Ha, I.; Ruvkun, G. Posttranscriptional regulation of the heterochronic gene *lin-14* by *lin-4* mediates temporal pattern formation in *C. elegans*. *Cell* **1993**, *75* (5), 855-862. DOI: 10.1016/0092-8674(93)90530-4 From NLM.
- (86) Perron, M. P.; Provost, P. Protein interactions and complexes in human microRNA biogenesis and function. *Front Biosci* **2008**, *13*, 2537-2547. DOI: 10.2741/2865 From NLM.
- (87) Rajagopalan, R.; Vaucheret, H.; Trejo, J.; Bartel, D. P. A diverse and evolutionarily fluid set of microRNAs in *Arabidopsis thaliana*. *Genes Dev* **2006**, *20* (24), 3407-3425. DOI: 10.1101/gad.1476406 From NLM.
- (88) Rajewsky, N. microRNA target predictions in animals. *Nat Genet* **2006**, *38 Suppl*, S8-13. DOI: 10.1038/ng1798 From NLM.
- (89) Berezikov, E.; Guryev, V.; van de Belt, J.; Wienholds, E.; Plasterk, R. H.; Cuppen, E. Phylogenetic shadowing and computational identification of human microRNA genes. *Cell* **2005**, *120* (1), 21-24. DOI: 10.1016/j.cell.2004.12.031 From NLM.
- (90) Bartel, D. P. MicroRNAs: genomics, biogenesis, mechanism, and function. *Cell* **2004**, *116* (2), 281-297. DOI: 10.1016/s0092-8674(04)00045-5 From NLM.
- (91) Marson, A.; Levine, S. S.; Cole, M. F.; Frampton, G. M.; Brambrink, T.; Johnstone, S.; Guenther, M. G.; Johnston, W. K.; Wernig, M.; Newman, J.; et al. Connecting microRNA genes to the core transcriptional regulatory circuitry of embryonic stem cells. *Cell* **2008**, *134* (3), 521-533. DOI: 10.1016/j.cell.2008.07.020 From NLM.
- (92) Gutschner, T.; Diederichs, S. The hallmarks of cancer: a long non-coding RNA point of view. *RNA Biol* **2012**, *9* (6), 703-719. DOI: 10.4161/rna.20481 From NLM.
- (93) Croce, C. Oncogenes and Cancer. *The New England journal of medicine* **2008**, *358*, 502-511. DOI: 10.1056/NEJMra072367.
- (94) Konopka, J. B.; Watanabe, S. M.; Singer, J. W.; Collins, S. J.; Witte, O. N. Cell lines and clinical isolates derived from Ph1-positive chronic myelogenous leukemia patients express c-abl proteins with a common structural alteration. *Proc Natl Acad Sci U S A* **1985**, *82* (6), 1810-1814. DOI: 10.1073/pnas.82.6.1810 From NLM.

- (95) Tsujimoto, Y.; Jaffe, E.; Cossman, J.; Gorham, J.; Nowell, P. C.; Croce, C. M. Clustering of breakpoints on chromosome 11 in human B-cell neoplasms with the t(11;14) chromosome translocation. *Nature* **1985**, *315* (6017), 340-343. DOI: 10.1038/315340a0 From NLM.
- (96) Sherr, C. J. Principles of tumor suppression. *Cell* **2004**, *116* (2), 235-246. DOI: 10.1016/s0092-8674(03)01075-4 From NLM.
- (97) Volinia, S.; Calin, G. A.; Liu, C. G.; Ambs, S.; Cimmino, A.; Petrocca, F.; Visone, R.; Iorio, M.; Roldo, C.; Ferracin, M.; et al. A microRNA expression signature of human solid tumors defines cancer gene targets. *Proc Natl Acad Sci U S A* **2006**, *103* (7), 2257-2261. DOI: 10.1073/pnas.0510565103 From NLM.
- (98) Liu, L.; Yu, X.; Guo, X.; Tian, Z.; Su, M.; Long, Y.; Huang, C.; Zhou, F.; Liu, M.; Wu, X.; et al. miR-143 is downregulated in cervical cancer and promotes apoptosis and inhibits tumor formation by targeting Bcl-2. *Mol Med Rep* **2012**, *5* (3), 753-760. DOI: 10.3892/mmr.2011.696 From NLM.
- (99) Borralho, P. M.; Kren, B. T.; Castro, R. E.; da Silva, I. B.; Steer, C. J.; Rodrigues, C. M. MicroRNA-143 reduces viability and increases sensitivity to 5-fluorouracil in HCT116 human colorectal cancer cells. *Febs j* **2009**, *276* (22), 6689-6700. DOI: 10.1111/j.1742-4658.2009.07383.x From NLM.
- (100) Karimi, L.; Mansoori, B.; Shanebandi, D.; Mohammadi, A.; Aghapour, M.; Baradaran, B. Function of microRNA-143 in different signal pathways in cancer: New insights into cancer therapy. *Biomed Pharmacother* **2017**, *91*, 121-131. DOI: 10.1016/j.biopha.2017.04.060 From NLM.
- (101) Tavanafar, F.; Safaralizadeh, R.; Hosseinpour-Feizi, M. A.; Mansoori, B.; Shanebandi, D.; Mohammadi, A.; Baradaran, B. Restoration of miR-143 expression could inhibit migration and growth of MDA-MB-468 cells through down-regulating the expression of invasion-related factors. *Biomed Pharmacother* **2017**, *91*, 920-924. DOI: 10.1016/j.biopha.2017.04.119 From NLM.
- (102) Xu, B.; Niu, X.; Zhang, X.; Tao, J.; Wu, D.; Wang, Z.; Li, P.; Zhang, W.; Wu, H.; Feng, N.; et al. miR-143 decreases prostate cancer cells proliferation and migration and enhances their sensitivity to docetaxel through suppression of KRAS. *Mol Cell Biochem* **2011**, *350* (1-2), 207-213. DOI: 10.1007/s11010-010-0700-6 From NLM.

- (103) Green, A. R.; Aleskandarany, M. A.; Agarwal, D.; Elsheikh, S.; Nolan, C. C.; Diez-Rodriguez, M.; Macmillan, R. D.; Ball, G. R.; Caldas, C.; Madhusudan, S.; et al. MYC functions are specific in biological subtypes of breast cancer and confers resistance to endocrine therapy in luminal tumours. *Br J Cancer* **2016**, *114* (8), 917-928. DOI: 10.1038/bjc.2016.46 From NLM.
- (104) Guo, Q.; Dong, B.; Nan, F.; Guan, D.; Zhang, Y. 5-Aminolevulinic acid photodynamic therapy in human cervical cancer via the activation of microRNA-143 and suppression of the Bcl-2/Bax signaling pathway. *Mol Med Rep* **2016**, *14* (1), 544-550. DOI: 10.3892/mmr.2016.5248 From NLM.
- (105) Chen, Y.; Ma, C.; Zhang, W.; Chen, Z.; Ma, L. Down regulation of miR-143 is related with tumor size, lymph node metastasis and HPV16 infection in cervical squamous cancer. *Diagn Pathol* **2014**, *9*, 88. DOI: 10.1186/1746-1596-9-88 From NLM.
- (106) Hosseinihli, N.; Zeinali, T.; Hosseinihli, N.; Karimi, L.; Shanebandi, D.; Mansoori, B.; Mohammadi, A.; Kazemi, T.; Hajiasgharzadeh, K.; Baradaran, B. Restoration of miRNA-143 Expression Inhibits Growth and Migration of MKN-45 Gastric Cancer Cell Line. *Adv Pharm Bull* **2022**, *12* (1), 183-190. DOI: 10.34172/apb.2022.020 From NLM.
- (107) Wu, Y.; Wang, Z.; Han, L.; Guo, Z.; Yan, B.; Guo, L.; Zhao, H.; Wei, M.; Hou, N.; Ye, J.; et al. PRMT5 regulates RNA m6A demethylation for doxorubicin sensitivity in breast cancer. *Mol Ther* **2022**, *30* (7), 2603-2617. DOI: 10.1016/j.ymthe.2022.03.003 From NLM.
- (108) Vatsyayan, R.; Chaudhary, P.; Lelsani, P. C.; Singhal, P.; Awasthi, Y. C.; Awasthi, S.; Singhal, S. S. Role of RLIP76 in doxorubicin resistance in lung cancer. *Int J Oncol* **2009**, *34* (6), 1505-1511. DOI: 10.3892/ijo\_00000279 From NLM.
- (109) Wang, T.; Tang, J.; Yang, H.; Yin, R.; Zhang, J.; Zhou, Q.; Liu, Z.; Cao, L.; Li, L.; Huang, Y.; et al. Effect of Apatinib Plus Pegylated Liposomal Doxorubicin vs Pegylated Liposomal Doxorubicin Alone on Platinum-Resistant Recurrent Ovarian Cancer: The APPROVE Randomized Clinical Trial. *JAMA Oncol* **2022**, *8* (8), 1169-1176. DOI: 10.1001/jamaoncol.2022.2253 From NLM.

- (110) Rosenberg, J. E.; Carroll, P. R.; Small, E. J. Update on chemotherapy for advanced bladder cancer. *J Urol* **2005**, *174* (1), 14-20. DOI: 10.1097/01.ju.0000162039.38023.5f From NLM.
- (111) Udhain, A.; Skubitz, K. M.; Northfelt, D. W. Pegylated liposomal doxorubicin in the treatment of AIDS-related Kaposi's sarcoma. *Int J Nanomedicine* **2007**, *2* (3), 345-352. From NLM.
- (112) Lai, C.; Cole, D. E.; Steinberg, S. M.; Lucas, N.; Dombi, E.; Melani, C.; Roschewski, M.; Balis, F.; Widemann, B. C.; Wilson, W. H. Doxorubicin pharmacokinetics and toxicity in patients with aggressive lymphoma and hepatic impairment. *Blood Adv* **2023**, *7* (4), 529-532. DOI: 10.1182/bloodadvances.2022007431 From NLM.
- (113) Roti Roti, E. C.; Leisman, S. K.; Abbott, D. H.; Salih, S. M. Acute doxorubicin insult in the mouse ovary is cell- and follicle-type dependent. *PLoS One* **2012**, *7* (8), e42293. DOI: 10.1371/journal.pone.0042293 From NLM.
- (114) Zhao, S.; Minh, L. V.; Li, N.; Garamus, V. M.; Handge, U. A.; Liu, J.; Zhang, R.; Willumeit-Römer, R.; Zou, A. Doxorubicin hydrochloride-oleic acid conjugate loaded nanostructured lipid carriers for tumor specific drug release. *Colloids Surf B Biointerfaces* **2016**, *145*, 95-103. DOI: 10.1016/j.colsurfb.2016.04.027 From NLM.
- (115) Carvalho, C.; Santos, R. X.; Cardoso, S.; Correia, S.; Oliveira, P. J.; Santos, M. S.; Moreira, P. I. Doxorubicin: the good, the bad and the ugly effect. *Curr Med Chem* **2009**, *16* (25), 3267-3285. DOI: 10.2174/092986709788803312 From NLM.
- (116) Jawad, B.; Poudel, L.; Podgornik, R.; Steinmetz, N. F.; Ching, W. Y. Molecular mechanism and binding free energy of doxorubicin intercalation in DNA. *Phys Chem Chem Phys* **2019**, *21* (7), 3877-3893. DOI: 10.1039/c8cp06776g From NLM.
- (117) Tacar, O.; Sriamornsak, P.; Dass, C. R. Doxorubicin: an update on anticancer molecular action, toxicity and novel drug delivery systems. *J Pharm Pharmacol* **2013**, *65* (2), 157-170. DOI: 10.1111/j.2042-7158.2012.01567.x From NLM.
- (118) Gabani, M.; Castañeda, D.; Nguyen, Q. M.; Choi, S. K.; Chen, C.; Mapara, A.; Kassan, A.; Gonzalez, A. A.; Khataei, T.; Ait-Aissa, K.; et al. Association of Cardiotoxicity With Doxorubicin and Trastuzumab: A Double-Edged Sword in Chemotherapy. *Cureus* **2021**, *13* (9), e18194. DOI: 10.7759/cureus.18194 From NLM.



- (119) Agudelo, D.; Bourassa, P.; Bérubé, G.; Tajmir-Riahi, H. A. Intercalation of antitumor drug doxorubicin and its analogue by DNA duplex: structural features and biological implications. *Int J Biol Macromol* **2014**, *66*, 144-150. DOI: 10.1016/j.ijbiomac.2014.02.028 From NLM.
- (120) Agudelo, D.; Bourassa, P.; Bérubé, G.; Tajmir-Riahi, H.-A. Intercalation of antitumor drug doxorubicin and its analogue by DNA duplex: Structural features and biological implications. *International Journal of Biological Macromolecules* **2014**, *66*, 144-150. DOI: <https://doi.org/10.1016/j.ijbiomac.2014.02.028>.
- (121) Chittipolu, A. Overview on the Side Effects of Doxorubicin. In *Advances in Precision Medicine Oncology*, Hilal, A., Bassam Abdul Rasool, H. Eds.; IntechOpen, 2020; p Ch. 10.
- (122) Speth, P. A.; van Hoesel, Q. G.; Haanen, C. Clinical pharmacokinetics of doxorubicin. *Clin Pharmacokinet* **1988**, *15* (1), 15-31. DOI: 10.2165/00003088-198815010-00002 From NLM.
- (123) Akkus Sut, P.; Tunc, C. U.; Culha, M. Lactose-modified DNA tile nanostructures as drug carriers. *J Drug Target* **2016**, *24* (8), 709-719. DOI: 10.3109/1061186x.2016.1144059 From NLM.
- (124) Costa, D. F.; Sarisozen, C.; Torchilin, V. P. Synthesis of Doxorubicin and miRNA Stimuli-Sensitive Conjugates for Combination Therapy. *Methods Mol Biol* **2019**, *1974*, 99-109. DOI: 10.1007/978-1-4939-9220-1\_8 From NLM.
- (125) Silva, E. F.; Bazoni, R. F.; Ramos, E. B.; Rocha, M. S. DNA-doxorubicin interaction: New insights and peculiarities. *Biopolymers* **2017**, *107* (3). DOI: 10.1002/bip.22998 From NLM.
- (126) Park, C.-M.; Xian, M. Chapter Eight - Use of Phosphorodithioate-Based Compounds as Hydrogen Sulfide Donors. In *Methods in Enzymology*, Cadenas, E., Packer, L. Eds.; Vol. 554; Academic Press, 2015; pp 127-142.
- (127) Ramachandran, V.; Chen, X. Degradation of microRNAs by a family of exoribonucleases in Arabidopsis. *Science* **2008**, *321* (5895), 1490-1492. DOI: 10.1126/science.1163728 From NLM.
- (128) Zhang, Z.; Qin, Y. W.; Brewer, G.; Jing, Q. MicroRNA degradation and turnover: regulating the regulators. *Wiley Interdiscip Rev RNA* **2012**, *3* (4), 593-600. DOI: 10.1002/wrna.1114 From NLM.

- (129) Soundararajan, S.; Wang, L.; Sridharan, V.; Chen, W.; Courtenay-Luck, N.; Jones, D.; Spicer, E. K.; Fernandes, D. J. Plasma membrane nucleolin is a receptor for the anticancer aptamer AS1411 in MV4-11 leukemia cells. *Mol Pharmacol* **2009**, *76* (5), 984-991. DOI: 10.1124/mol.109.055947 From NLM.
- (130) Chen, Z.; Xu, X. Roles of nucleolin. Focus on cancer and anti-cancer therapy. *Saudi Med J* **2016**, *37* (12), 1312-1318. DOI: 10.15537/smj.2016.12.15972 From NLM.
- (131) Lohlamoh, W.; Soontornworajit, B.; Rotkrua, P. Anti-Proliferative Effect of Doxorubicin-Loaded AS1411 Aptamer on Colorectal Cancer Cell. *Asian Pac J Cancer Prev* **2021**, *22* (7), 2209-2219. DOI: 10.31557/apjcp.2021.22.7.2209 From NLM.
- (132) Mazza, T.; Mazzocchi, G.; Fusilli, C.; Capocéfalo, D.; Panza, A.; Biagini, T.; Castellana, S.; Gentile, A.; De Cata, A.; Palumbo, O.; et al. Multifaceted enrichment analysis of RNA-RNA crosstalk reveals cooperating micro-societies in human colorectal cancer. *Nucleic Acids Res* **2016**, *44* (9), 4025-4036. DOI: 10.1093/nar/gkw245 From NLM.
- (133) Kent, O. A.; Chivukula, R. R.; Mullendore, M.; Wentzel, E. A.; Feldmann, G.; Lee, K. H.; Liu, S.; Leach, S. D.; Maitra, A.; Mendell, J. T. Repression of the miR-143/145 cluster by oncogenic Ras initiates a tumor-promoting feed-forward pathway. *Genes Dev* **2010**, *24* (24), 2754-2759. DOI: 10.1101/gad.1950610 From NLM.
- (134) Akao, Y.; Kumazaki, M.; Shinohara, H.; Sugito, N.; Kuranaga, Y.; Tsujino, T.; Yoshikawa, Y.; Kitade, Y. Impairment of K-Ras signaling networks and increased efficacy of epidermal growth factor receptor inhibitors by a novel synthetic miR-143. *Cancer Sci* **2018**, *109* (5), 1455-1467. DOI: 10.1111/cas.13559 From NLM.
- (135) Yang, F.; Teves, S. S.; Kemp, C. J.; Henikoff, S. Doxorubicin, DNA torsion, and chromatin dynamics. *Biochim Biophys Acta* **2014**, *1845* (1), 84-89. DOI: 10.1016/j.bbcan.2013.12.002 From NLM.
- (136) Chaires, J. B.; Herrera, J. E.; Waring, M. J. Preferential binding of daunomycin to 5'ATCG and 5'ATGC sequences revealed by footprinting titration experiments. *Biochemistry* **1990**, *29* (26), 6145-6153. DOI: 10.1021/bi00478a006 From NLM.
- (137) Li, P.; Nijhawan, D.; Budihardjo, I.; Srinivasula, S. M.; Ahmad, M.; Alnemri, E. S.; Wang, X. Cytochrome c and dATP-dependent formation of Apaf-1/caspase-9



- complex initiates an apoptotic protease cascade. *Cell* **1997**, *91* (4), 479-489. DOI: 10.1016/s0092-8674(00)80434-1 From NLM.
- (138) Riedl, S. J.; Salvesen, G. S. The apoptosome: signalling platform of cell death. *Nat Rev Mol Cell Biol* **2007**, *8* (5), 405-413. DOI: 10.1038/nrm2153 From NLM.
- (139) Cory, S.; Adams, J. M. The Bcl2 family: regulators of the cellular life-or-death switch. *Nat Rev Cancer* **2002**, *2* (9), 647-656. DOI: 10.1038/nrc883 From NLM.
- (140) A Modified MTS Proliferation Assay for Suspended Cells to Avoid the Interference by Hydralazine and  $\beta$ -Mercaptoethanol. *ASSAY and Drug Development Technologies* **2021**, *19* (3), 184-190. DOI: 10.1089/adt.2020.1027.
- (141) Cory, A. H.; Owen, T. C.; Barltrop, J. A.; Cory, J. G. Use of an aqueous soluble tetrazolium/formazan assay for cell growth assays in culture. *Cancer Commun* **1991**, *3* (7), 207-212. DOI: 10.3727/095535491820873191 From NLM.
- (142) Schmittgen, T. D.; Zakrajsek, B. A.; Mills, A. G.; Gorn, V.; Singer, M. J.; Reed, M. W. Quantitative reverse transcription-polymerase chain reaction to study mRNA decay: comparison of endpoint and real-time methods. *Anal Biochem* **2000**, *285* (2), 194-204. DOI: 10.1006/abio.2000.4753 From NLM.
- (143) Wilhelm, J.; Pingoud, A. Real-time polymerase chain reaction. *Chembiochem* **2003**, *4* (11), 1120-1128. DOI: 10.1002/cbic.200300662 From NLM.
- (144) Wagner, E. M. Monitoring gene expression: quantitative real-time rt-PCR. *Methods Mol Biol* **2013**, *1027*, 19-45. DOI: 10.1007/978-1-60327-369-5\_2 From NLM.
- (145) McKinnon, K. M. Flow Cytometry: An Overview. *Curr Protoc Immunol* **2018**, *120*, 5.1.1-5.1.11. DOI: 10.1002/cpim.40 From NLM.
- (146) Riccardi, C.; Nicoletti, I. Analysis of apoptosis by propidium iodide staining and flow cytometry. *Nature Protocols* **2006**, *1* (3), 1458-1461. DOI: 10.1038/nprot.2006.238.
- (147) Casciola-Rosen, L.; Rosen, A.; Petri, M.; Schlissel, M. Surface blebs on apoptotic cells are sites of enhanced procoagulant activity: implications for coagulation events and antigenic spread in systemic lupus erythematosus. *Proc Natl Acad Sci U S A* **1996**, *93* (4), 1624-1629. DOI: 10.1073/pnas.93.4.1624 From NLM.
- (148) Koopman, G.; Reutelingsperger, C. P.; Kuijten, G. A.; Keehnen, R. M.; Pals, S. T.; van Oers, M. H. Annexin V for flow cytometric detection of phosphatidylserine

expression on B cells undergoing apoptosis. *Blood* **1994**, 84 (5), 1415-1420. From NLM.

(149) Vermes, I.; Haanen, C.; Steffens-Nakken, H.; Reutelingsperger, C. A novel assay for apoptosis. Flow cytometric detection of phosphatidylserine expression on early apoptotic cells using fluorescein labelled Annexin V. *J Immunol Methods* **1995**, 184 (1), 39-51. DOI: 10.1016/0022-1759(95)00072-i From NLM.



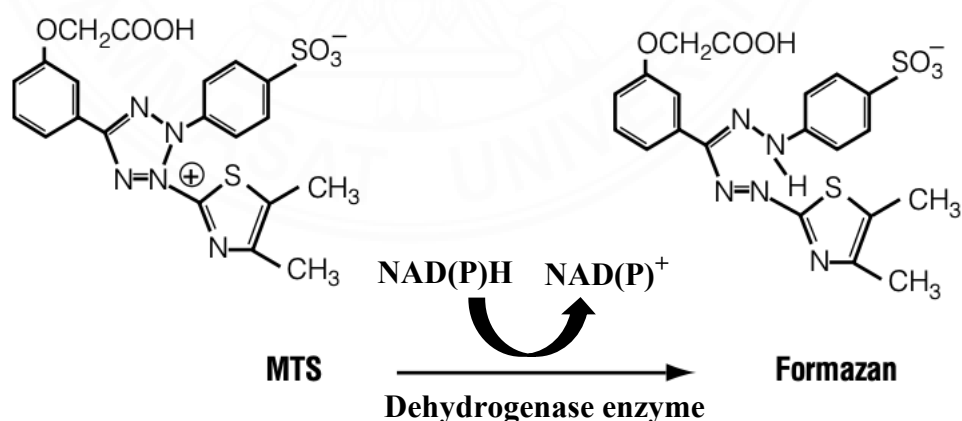
The seal of Thammasat University is a circular emblem. It features a central five-tiered umbrella (parasol) with a lotus flower at its base. Above the lotus is a horizontal bar with five lines. The entire emblem is surrounded by a circular border containing the university's name in Thai script at the top and "THAMMASAT UNIVERSITY" in English at the bottom, separated by small floral motifs.

## **APPENDICES**

## APPENDIX A

### CELL PROLIFERATION

The CellTiter 96<sup>®</sup> AQueous One Solution Cell Proliferation Assay or MTS Assay (Promega, USA) is a method using colorimetric analysis for detecting the quantity of live cells in assays for cytotoxicity or proliferation. Tetrazolium compounds [3-(4,5-dimethylthiazol-2-yl)-5-(3-carboxymethoxyphenyl)-2-(4-sulfophenyl)-2H-tetrazolium, inner salt; MTS] could be changed by NAD(P)H-dependent oxidoreductase enzymes generated in mitochondria in living cells into colorful formazan in proportion to the metabolic activity of mitochondrial enzymes. This Solution includes a new tetrazolium compound (MTS) and PES, or phenazine ethosulfate, is an electron coupling reagent. The combination of PES and MTS results in a stable solution due to PES's enhanced chemical stability. A spectrophotometer could be used to measure the amount of formazan generated to determine the quantity of cells present. The MTS reagent is given directly to the cultivated cells, and after a predefined period time 1 hour, absorbance is measured at 490 nm using a microplate reader.<sup>140, 141</sup>



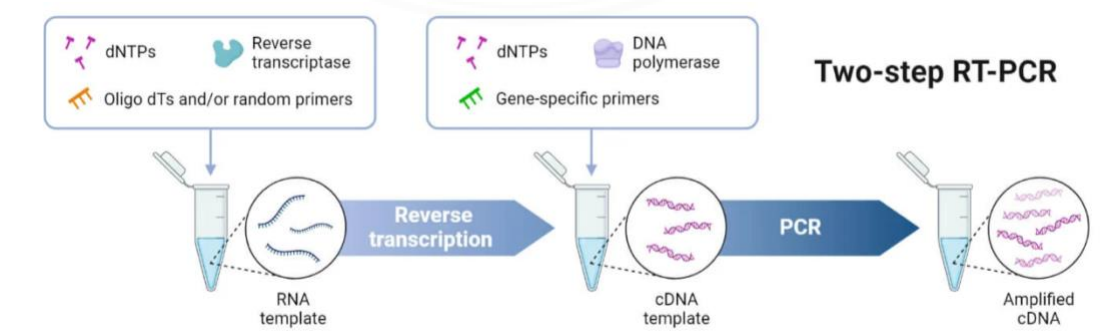
Structures of MTS tetrazolium and its formazan product.<sup>141</sup>

## APPENDIX B

### QUANTITATIVE REAL TIME POLYMERASE CHAIN REACTION

One technique for identifying and quantifying RNA is the quantitative reverse transcription polymerase chain reaction, or RT-qPCR. The starting material for complementary DNA (cDNA) is total RNA, commonly referred to as messenger RNA (mRNA). The qPCR process then makes use of the cDNA as a template. An alternative to the conventional PCR method for measuring DNA or RNA in a sample is called RT-qPCR. Sequence-specific primers can be utilized to determine the number of replicas of a particular DNA or RNA sequence. Quantification could be accomplished by determining the amount of amplified product at each PCR cycle stage. Amplification happens sooner in the cycle when a certain sequence (DNA or RNA) is abundant in the sample; when the sequence is sparse, amplification occurs later in the cycle. For measuring the amplified product, fluorescent probes or fluorescent DNA-binding dyes are utilized, and real-time PCR instruments detect fluorescence while completing the thermal cycling necessary for the PCR process<sup>142, 143</sup>.

Two-step RT-qPCR consists of two distinct reactions: first-strand cDNA synthesis (RT) and qPCR amplification of a portion of the resultant cDNA in a different tube. Consequently, many genes can be found in a single RNA sample using two-step RT-qPCR. The separation of RT and PCR processes allows for the adjustment of reaction parameters for each step<sup>144</sup>.



Two-step RT-PCR diagram (figure made in BioRender from AAT Bioquest, Inc. All Rights Reserved.).

## APPENDIX C

### FLOW CYTOMETRY

Flow cytometry is a technique that uses various types of parameters to evaluate single cells in solution in real-time. The scattered and fluorescent light signals generated by lasers, which are used as light sources in flow cytometers, are read by detectors such as photodiodes or photomultiplier tubes. It is a potent tool having uses in cancer biology, bacteriology, immunology, molecular biology, and infectious disease monitoring. Its tremendous advances over the past three decades have made it possible to study the immune system and other facets of cell biology in unprecedented detail<sup>145</sup>.

Flow cytometry approaches have had a considerable influence on studies of cellular apoptosis. Propidium iodide (PI) is commonly used in combination with Annexin V to evaluate whether cells are alive, apoptotic, or necrotic by observing changes in plasma membrane integrity and permeability<sup>146</sup>. Characteristics of the apoptotic program include loss of attachment and asymmetry of the plasma membrane, nuclear and cytoplasmic condensation, as well as DNA breaking by internucleosomes. A first indication is the loss of the plasma membrane. Phospholipid phosphatidylserine (PS) translocates from the inner to the outer leaflet of the plasma membrane in apoptotic cells, affording PS exposure to the surrounding cellular environment<sup>147</sup>. Annexin V is a  $\text{Ca}^{2+}$ -dependent phospholipid-binding protein that attaches to cells with exposed PS and has a high affinity for PS. Annexin V can be coupled with fluorochromes such as FITC<sup>148</sup>. For example, live cells are FITC Annexin V negative and PI negative; necrotic cells are PI positive and FITC Annexin V negative; early apoptotic cells are FITC Annexin V positive and PI negative; and late apoptotic or dead cells are both FITC Annexin V and PI positive<sup>149</sup>.

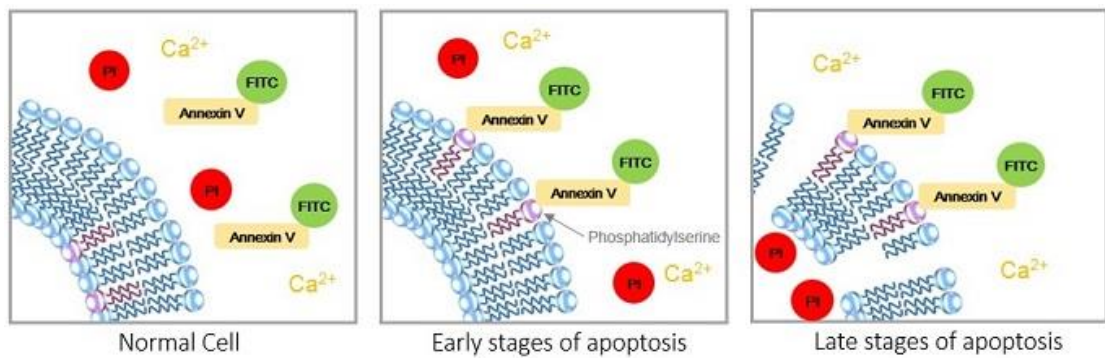
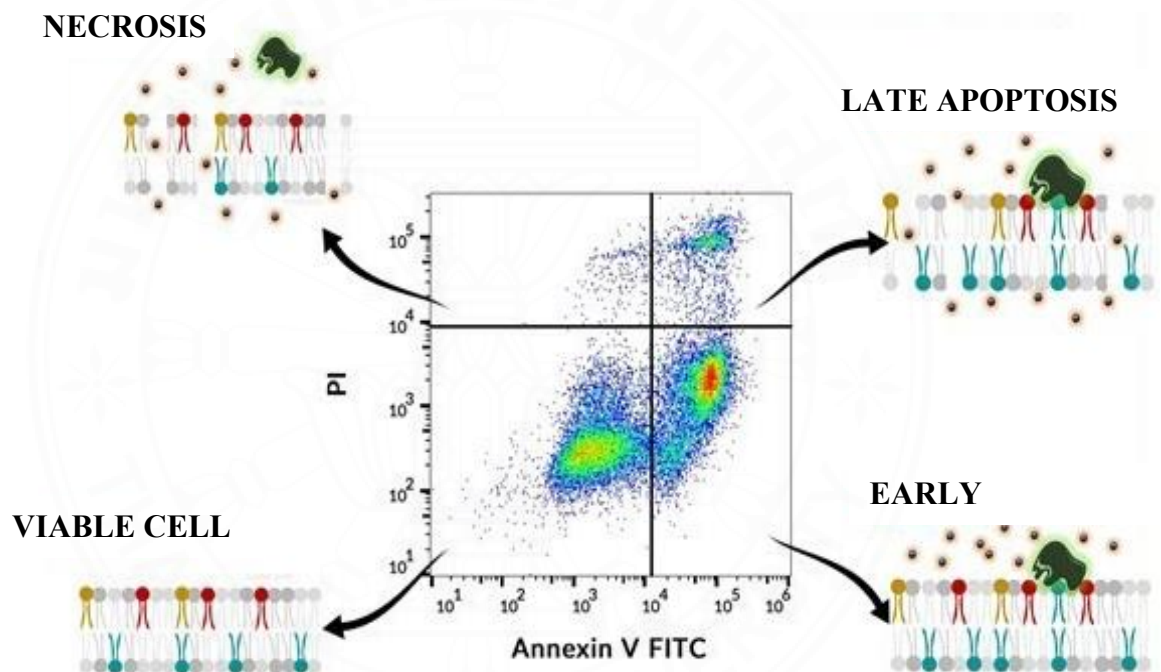


(Figure made by DOJINDO Laboratories)



Annexin V/PI staining for measuring apoptosis by flow cytometry. (figure made by Animated biology with Arpan)

## APPENDIX D

### PREPARATION FOR EXPERIMENTAL REAGENT

#### electrophoresis

##### 10% APS

Ammonium persulfate	0.10 g
---------------------	--------

Dissolve ammonium persulfate in 1 mL of DI water.

##### 5X TBE buffer

Tris-Base (Tris(hydroxymethyl)aminomethane)	54 g
Boric acid	27.5 g
EDTA disodium salt	3.75 g

Dissolve Tris-Base, Boric acid, and EDTA disodium in 1000 mL of DI water.

##### 10% SDS

Sodium dodecyl sulfate	10 g
------------------------	------

Dissolve SDS in 1 mL of DI water.

##### 1.5 M Tris-HCl, pH 8.8

Tris-Base (Tris(hydroxymethyl)aminomethane)	18.16 g
---	---------

Adjust the pH to 8.8 with 6 N HCl and add DI water to 100 mL.

##### 0.5 M Tris-HCl, pH 6.8

Tris-Base (Tris(hydroxymethyl)aminomethane)	6 g
---	-----

Adjust the pH to 6.8 with 6 N HCl and add DI water to 100 mL.

##### Running buffer stock 10x pH 8.3

25 mM Tris-Base (Tris(hydroxymethyl)aminomethane)	30.30 g
192 mM Glycine	144.10 g
10% SDS	10 g

Adjust the pH to 8.3 with 6 N HCl and add DI water to 1000 mL.



**1x Running buffer**

10x Running buffer pH 8.3	100 mL
DI water	900 mL

**Transfer buffer or Towbin buffer stock 10x pH 8.3**

25 mM Tris-Base (Tris(hydroxymethyl)aminomethane)	30.30 g
192 mM Glycine	144.10 g

Adjust the pH to 8.3 with 6 N HCl and add DI water to 1000 mL.

**1x Transfer buffer**

10x Transfer buffer pH 8.3	100 mL
Methanol	200 mL
DI water	700 mL

**10% Polyacrylamide gel**

30% Polyacrylamide	2 mL
5X TBE	1.2 mL
10% APS	50 $\mu$ L
TEMED	5 $\mu$ L
DI water	2.8 mL

**15% Polyacrylamide gel**

30% Polyacrylamide	1 mL
5X TBE	400 $\mu$ L
10% APS	20 $\mu$ L
TEMED	2 $\mu$ L
DI water	600 $\mu$ L

**4% Polyacrylamide gel**

30% Polyacrylamide	1.3 mL
0.5 M Tris-HCl, pH 8.8	2.5 mL
10% SDS	100 $\mu$ L

10% APS	100 $\mu$ L
TEMED	20 $\mu$ L
DI water	6.0 mL

### 12% Polyacrylamide gel

30% Polyacrylamide	8 mL
1.5 M Tris-HCl, pH 8.8	5.2 mL
10% SDS	200 $\mu$ L
10% APS	200 $\mu$ L
TEMED	40 $\mu$ L
DI water	6.4 mL

### Reverse Transcription (RT) master mix

100mM dNTPs (with dTTP)	0.15 $\mu$ L
MultiScribe™ Reverse Transcriptase, 50U/ $\mu$ L	1 $\mu$ L
10X Reverse Transcription Buffer	1.50 $\mu$ L
RNase Inhibitor, 20U/ $\mu$ L	0.19 $\mu$ L
Nuclease-free water	4.16 $\mu$ L

### RT reaction

RT master mix	7 $\mu$ L
Total RNA 10 ng	1 $\mu$ L
Nuclease-free water	4 $\mu$ L
RT miR-143 Primer	3 $\mu$ L

### PCR reaction

TaqMan MicroRNA Assay (20X)	1 $\mu$ L
TaqMan 2X Universal PCR Master Mix, No AmpErase UNG <sup>a</sup>	10 $\mu$ L
RT reaction product	1.33 $\mu$ L
Nuclease-free water	7.67 $\mu$ L

## BIOGRAPHY

Name	Miss Khanittha Laowichuwakonnukul
Date of Birth	January 17, 1997
Educational Attainment	2019: Bachelor of Science (Chemistry) Rajamangala University of Technology Thanyaburi, Thailand
Scholarship	2021-2022: Teaching Assistant Scholarship of Thammasat university

### Publications

1. Vichitsakul, K.; Laowichuwakonnukul, K.; Soontornworajit, B.; Poomipark, N.; Itharat, A.; Rotkrua, P. Anti-proliferation and induction of mitochondria-mediated apoptosis by *Garcinia hanburyi* resin in colorectal cancer cells. *Heliyon* 2023, 9 (6), e16411. DOI: 10.1016/j.heliyon.2023.e16411 From NLM.

### Presentation

1. Laowichuwakonnukul, K., Soontornwarajit b., Rotkrua P. Development of a molecular hybrid of microRNA and aptamer for regulating the proliferation of colorectal cancer cell. Young Scientist Award 2023, 23 August 2023. Stang Mongkolsuk Conference Room, Faculty of Science, Mahidol University, Thailand.
2. Laowichuwakonnukul, K., Soontornwarajit b., Rotkrua P. Targeted delivery of miR-143 and Doxorubicin to SW480 cells using a molecular hybrid of microRNA and aptamer. MBSJ International Conference 2023, 6-8 December 2023. Kobe International Exhibition Hall, Kobe, Japan.